International Journal of Solids and Structures 59 (2015) 1–17

Contents lists available at ScienceDirect

International Journal of Solids and Structures

journal homepage: www.elsevier.com/locate/ijsolstr

Continuum and discrete models for structures including (quasi-) inextensible elasticae with a view to the design and modeling of composite reinforcements

M.V. d'Agostino [a], I. Giorgio [b,c], L. Greco [b], A. Madeo [a,b,*], P. Boisse [a]

[a] INSA de Lyon, 20 avenue Albert Einstein, 69621 Villeurbanne cedex, France
[b] MEMOCS Int. Research Center for the Mathematics and Mechanics of Complex Systems, Università dell'Aquila, Italy
[c] Dipartimento di Ingegneria Strutturale e Geotecnica, Università Sapienza di Roma, Via Eudossiana 18, 00184 Roma, Italy

ARTICLE INFO

Article history:
Received 14 June 2014
Received in revised form 2 October 2014
Available online 31 December 2014

Keywords:
Discrete models
Continuum second gradient models
Fibrous composite reinforcements
Bias extension test

ABSTRACT

Inspired by some composite fiber reinforcements used in aeronautical engineering and by the need of conceiving new metamaterials, some discrete models including (quasi-) inextensible elasticae are considered. A class of continuum models approximately describing the macroscopic mechanical behavior of introduced structures is then heuristically proposed. Some of these continuum models can be regarded as a special kind of second-gradient elastic media, in which the higher-gradient elasticity is conferred by the flexural stiffnesses of elasticae constituting the microscopic lattice. The discrete models are studied by means of suitably tailored numerical codes designed to avoid numerical instabilities and locking and a comparison of discrete versus continuum models is attempted. The obtained results show that the theory of generalized continua may be useful in some engineering applications and it plays a relevant role in the mechanics of woven composites. The introduced discrete and continuum models are used to describe the so-called bias extension test on woven fabrics and it is shown that a good choice to correctly reproduce the targeted phenomenology is to use a second gradient continuum theory. However, as discussed throughout the paper, in the context of rigorous micro–macro identification procedures there still remain many open problems to be solved, especially when dealing with systems subjected to particular constraints, such as inextensibility.

1. Introduction

As it happens for every mathematical model intended to be used for natural phenomena, the continuum model of deformable bodies developed following Cauchy's point of view, although may be very effective to carefully describe a wealthy of systems, cannot be universally applied. As a matter of fact, already at a very early stage of Cauchy formulation of the basic ideas of continuum models, Piola (in preparation), with a stringent mathematical study, analyzed its limits and proposed some more general models which are nowadays widely used. More than one century later Piola's ideas resurfaced (for a discussion of these phenomena of re-discovery the interested reader should consult the work by Russo (2004)) and a group of scientists (Koiter, 1964; Mindlin and Tiersten, 1962; Mindlin, 1964, 1965; Mindlin and Eshel, 1968; Toupin, 1962, 1964; Green and Rivlin, 1964a,b,c, 1965; Germain, 1973b,a; Eringen, 2001; Eringen and Suhubi, 1964,) reformulated, accepted and understood the objections and observations pushed forward by Piola and restarted and developed his work. Although, for some reasons to be investigated, the impetus of this flow of ideas was relented until the beginning of XXI century, they are now flourishing and constitute those fields which are variously named as: generalized continuum models, multi-scale models, second or higher gradient (or higher grade) continua, microstructured continua, multipolar continua, enhanced continuum models and so on (see e.g. dell'Isola et al., in press; Pideri and Seppecher, 1997; Camar-Eddine and Seppecher, 2002, 2003; Bouchet and Brechet, 2009; Auffray et al., 2010; Auffray et al., in press; Svendsen et al., 2009; Neff and Forest, 2007).

In this paper we propose to show that such generalized continuum models can be useful to characterize mechanical systems composed by nearly inextensible fibers with relatively low bending stiffness. To these systems was dedicated the interesting work Spencer (1972), Spencer and Soldatos (2007), which represents an unavoidable reference in the field. Such work has been followed by several researchers (e.g. Qiu and Pence, 1997; Holzapfel et al., 2000; Merodio and Ogden, 2005) and extended to the case of

* Corresponding author at: INSA de Lyon, 20 avenue Albert Einstein, 69621 Villeurbanne cedex, France. Tel.: +33 (0)4 72438463; fax: +33 (0)4 72438521.
E-mail address: angela.madeo@insa-lyon.fr (A. Madeo).

http://dx.doi.org/10.1016/j.ijsolstr.2014.12.014
0020-7683/

statistically distributed families of fibers, (e.g. Lanir, 1983; Federico et al., 2004; Gasser et al., 2006; Federico and Herzog, 2008; Federico and Gasser, 2010) and porous media (e.g. Federico and Grillo, 2012; Tomic et al., 2014).

We start by presenting two discrete models which are inspired by, but do not exactly coincide with, some woven fabrics constituted by nearly inextensible fibers (see e.g. Boisse, 2012; Cao et al., 2008; Ferretti et al., 2013):

- A simple two-dimensional structure consisting of (long) elasticae (as models for nearly inextensible fibers) connected to each other by means of perfect internal pivots, in the manner of a pantographic lattice (the internal pivots do not interrupt the continuity of the fibers). These fibers, and associated pivots, are assumed to be uniformly distributed in the plane. We assume that the fibers are (nearly-) inextensible elasticae with equal flexural stiffnesses. Once a corresponding homogenized model is introduced we get a generalization of Pipkin's theory of perfectly flexible inextensible nets with shear resistance (Pipkin, 1980; Pipkin, 1981; Pipkin, 1984; Steigmann and Pipkin, 1991), the latter manifesting itself as a dependence of the strain-energy function on the shear angle between intersecting fibers. This type of shear resistance vanishes in the present model of ideal pantographic lattices characterized by ideal pivots in which there is no concentrated rotational elastic stiffness. Similar structures that exhibit such *floppy modes* (modes with vanishing associated energy) are discussed comprehensively in Kuznetsov (1991) and closely resemble those studied in Alibert et al. (2003). Here, we recall that (see dell'Isola and Steigmann, 2014) the compatibility of the first gradient of the deformation is shown to imply a direct connection between the *gradient of fiber shear* and the *fiber bending strains*: this effect is associated with the second gradient of deformation. Accordingly, the *pantographic substructure* leads naturally to a particular second-gradient continuum theory of elasticity. This is indeed a very particular generalized continuum, where no extra kinematical descriptor is introduced: the only difference of the model which we present here when compared with standard Cauchy continua consists in the introduction of second gradient of displacement as an independent variable in the constitutive equation for deformation energy.
- Another way to model a metamaterial with a microstructure consisting of nearly inextensible fibers is given by the introduction of local constraints in the discrete continuum model at the finite element (FE) level. More particularly, the elementary cell of the discretization is composed by standard quadrilateral elements with the addition of very stiff diagonal bar elements joining the opposite corner nodes (mimicking the behavior of fibers) with an axial stiffness which is very high with respect to the in-plane stiffness of the considered FE. Basically, this strategy consists in a penalty for the deformations along particular directions in the plane of the material, (TPM, Truss Penalty Method). This strategy is a weak version of the one presented in Hamila and Boisse (2013) in which the authors have implicitly imposed the inextensibility constraint locally at each Gauss points of the FE. The strategy presented in this work imposes the inextensibility constraint globally at the element level. Moreover, in this way it is possible to generalize the method for a n-family of constrained directions. In this paper we present a 2-family fiber reinforcement that in the following is denoted by TPM-2 and which will be seen to be useful for the description of so-called bias extension test.

On the basis of the informations obtained by means of the considered discrete models we finally investigate the continuum description of fibrous composite reinforcements and we end up with the conclusion that a second gradient theory is indeed necessary in order to account for the bending stiffness of fibers at the microscopic level. We are of course aware that the particular second gradient continuous model which we present here may not be general enough to describe carefully all the macroscopic phenomenology of considered mechanical systems: we may need to introduce continua endowed with microstructure fields (see e.g. Eringen, 2001; dell'Isola et al., 1997, 1998) as, for instance, directors. Moreover, the most general constitutive modeling of 2D anisotropic structures made of flexible nets of fibers should rely on the methods based on the material symmetry groups (see e.g. Bouchet and Brechet, 2009; Eremeyev and Pietraszkiewicz, 2006; Eremeyev and Pietraszkiewicz, 2012). Inertia damage, plastic deformation or dislocation effects[1] are not included in the present model and would require the introduction of some extra kinematical descriptors in order to account for those phenomena of energy distribution, trapping and flow which were studied – in different contexts – in the papers (Carcaterra, 2002; Carcaterra and Akay, 2004; Culla et al., 2003; Ko et al., 2005; Luongo, 2001; Neff et al., 2013b; Madeo et al., 2013). The phenomenology of fibrous reinforcements is rich of instability and bifurcation phenomena due to the interest which has to be directed towards their large deformation configurations (see e.g. Bel et al., 2012; Boisse, 2012; Hamila et al., 2009; Yu et al., 2005; King et al., 2005). Indeed, one can observe wrinkling (see e.g. Boisse et al., 2011; King et al., 2005), plies and plastic deformations, etc.: for a comprehensive description of the relevant phenomenology see e.g. Bel et al. (2012), Boisse (2012), Cao et al. (2008), Ferretti et al. (2013), Indelicato (2008), Willems et al. (2008), Fetfatsidis et al. (2013) and Yu et al. (2005). One of the possible applications of the presented model could involve the study of the static and dynamic instabilities together with the analysis of the corresponding bifurcations: in this case many perturbation and numerical methods (see e.g. Luongo, 1991, 1995, 2001; Di Egidio et al., 2007;Reccia et al., 2012; Luongo et al., 1986; Contento and Luongo, 2013; Luongo and Pignataro, 1988; Pignataro and Luongo, 1994) applied to structures similar to the one considered in the present paper could represent a powerful tool.

When presenting the numerical simulations associated to the introduced continuum models, we will point out that some numerical errors related to the high contrast between the tensile stiffness and the bending stiffness of yarns may arise. These phenomena are known as tension locking phenomena (see e.g. Hamila and Boisse, 2013) and are mitigated here by choosing suitably refined meshes and finite elements of suitably high order. These numerical difficulties resemble and often parallel those already confronted for studying (eventually generalized) shell (Garusi et al., 2004; Cazzani and Lovadina, 1997; Cazzani and Ruge, 2012; Ciancio et al., 2006; Contro et al., 1988) and beam (Cuomo and Ventura, 2002; Contro et al., 1988; Cuomo et al., in press; Greco and Cuomo, 2013, 2014) models. In this context the results and methods presented in Ciancio et al. (2006), Contrafatto and Cuomo (2005), Cuomo and Contrafatto (2000), Cuomo and Ventura (1998), Hamila and Boisse (2013) and Badel et al. (2009) also seem to be able to supply useful tools.

2. Materials with strong contrast of the mechanical properties at the microscopic level

It is known (see e.g. Seppecher et al., 2011) that materials which have strong contrasts of the mechanical properties at the microscopic level are likely to behave as generalized continua when sub-

[1] one can think, for instance, to situations where the contact area between two fibers changes in time in either reversible or irreversible way (in this context it could be possible to use the methods presented e.g. in Badel et al. (2009), Cuomo and Contrafatto (2000), Oliveto and Cuomo (1988) and Cuomo and Nicolosi (2006)).

jected to particular loading and/or boundary conditions. It has been recently shown (see Ferretti et al., 2013) that a particular class of engineering materials, known as fibrous composite reinforcements, show exotic mechanical properties when considering particular loading conditions and kinematical constraints. Fibrous composite reinforcements are woven fabrics which present a very high tension stiffness in the warp and weft directions together with a very low shear stiffness. In other words, the yarns constituting such materials are very stiff in tension, while the angle variation between two superimposed yarns (warp and weft) can occur very easily. These characteristics make fibrous composite reinforcements a topical example to better understand which types of microstructures must be considered in order to obtain second or higher order continua at the homogenized level.

In virtue of the importance of the mechanical modeling of these materials for engineering, it is essential to establish which theoretical and numerical models must be adopted to better describe their macroscopic and mesoscopic properties.

Fig. 1 shows the macroscopic engineering component of fibrous composite reinforcement, its mesoscopic scale (warp and weft) and the microstructure of each yarn. We are interested here to the mesoscopic and macroscopic scale of such materials and we will try to model from a theoretical and a numerical point of view some peculiar deformation patterns of 2D woven composites at the scale of warp and weft and then at the scale of the whole engineering component. As already discussed, we propose here to address the modeling of the mechanical behavior of 2D fibrous composite reinforcements both by considering.

- discrete mechanical systems mimicking at best the characteristics of the underlying mesostructures,
- continuum models which are able to correctly catch the overall mechanical behavior of such systems.

We will show the limits of the considered discrete modeling while capturing from them some essential features which are needed to understand the correct way of exploiting generalized continuum theories via finite element methods.

In this paper, we target to reproduce a very common experimental test on woven composites which is known as bias extension test: we will use this example as a reference case for testing the efficacy of all the introduced discrete and continuum models. The bias extension test is a mechanical test which is widely used in the field of fibrous composite materials. This test is useful to characterize the mechanical behavior of woven fibrous composites undergoing large shear deformations.

The bias extension test is performed on rectangular samples of woven composites, with the height (in the loading direction) relatively greater (at least twice) than the width, and the yarns initially oriented at ±45-degrees with respect to the loading direction (see Fig. 2). The specimen is clamped at two ends: one end is maintained fixed and the second one is gradually displaced of a given amount. The relative displacement of the two ends of the specimen generates angle variations between the warp and weft. The deformed configuration consists of three different regions A, B and C, in which the shear angle between the yarns remains almost constant (see Fig. 3 and references Bel et al. (2012), Cao et al. (2008) and Harrison (2012)). More particularly, the fibers in regions C remain undeformed, i.e. the angle between fibers remains at 45° also after deformation. As far as considering the other regions A and B, the angle between fibers becomes much smaller than 45°, but it keeps almost constant in each region. The main characteristics of the bias extension test are summarized in Fig. 3 in which both the undeformed and deformed shapes of the considered specimen are schematically depicted. In Ferretti et al. (2013) it has also been put in evidence that another important phenomenological aspect of the bias extension test must be taken into account. In particular, at the transition lines between two different regions at constant shear angle the presence of thin transition layers can be identified which allow a smooth transition from a region with constant shear angle to the adjacent one (see Fig. 4). These layers will be called shear transition layers and their thickness can be associated to the gradient of shear angle variation between yarns (or equivalently to the in-plane bending stiffness of the yarns). It is clear that a complete predictive model of the bias extension test must necessarily include an accurate description of such shear transition layers.

In the reminder of this paper, we will propose different discrete and continuum models for the description of the bias extension test and we will point out which ones of the main characteristics of this test are well described (or not) in each model.

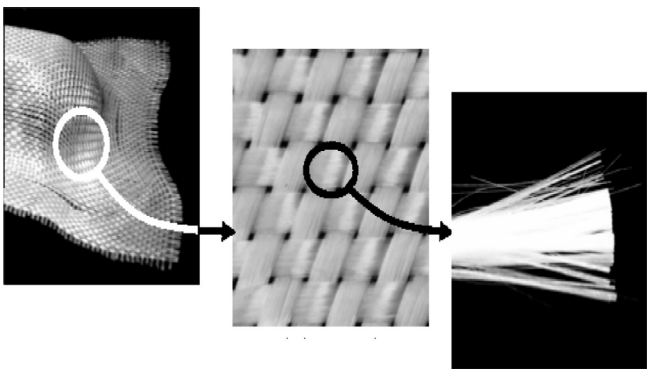

Fig. 1. Macroscopic, mesoscopic and microscopic scale of a woven fabric.

3. Discrete mechanical systems including strong contrast at lower scales

As it has been previously discussed, fibrous composite reinforcements exhibit a strong contrast between the tension and the shear stiffnesses at the mesoscopic level. In this section we propose two different discrete systems which can be built-up by means of available softwares and which include the possibility of accounting for such kinds of strong contrasts.

3.1. Pantographic lattices

As a first example of discrete modeling of fibrous networks, we introduce a modular pantographic structure which can be described, at the mesoscopic level, as a structure constituted by nearly inextensible but flexible Euler–Bernoulli beams connected by pivots at their intersection points. It is worth noting that the considered structure is different from a truss-like structure since the internal pivots do not interrupt the continuity of each beam. In other words, in presence of appropriate loading and boundary conditions, the bending moment in each beam is not vanishing as in truss structures, but it is instead fundamental to characterize the global structural response. The considered beams have an elliptical cross section, in which the major and minor axis are respectively denoted by D_1 and D_2: the major axis lies in the considered plane and the orientation of the beams is at ±45° with respect to the global reference frame (see Fig. 5). The yarns are supposed to be constituted by carbon fibers and the used elastic and geometric parameters are summarized in Table 1.

The considered beams are linear-elastic beams i.e. no geometrical nor material linearities are included in this model. We assume that external actions and external constraints are applied at intersection nodes only. In the next section we will show numerical

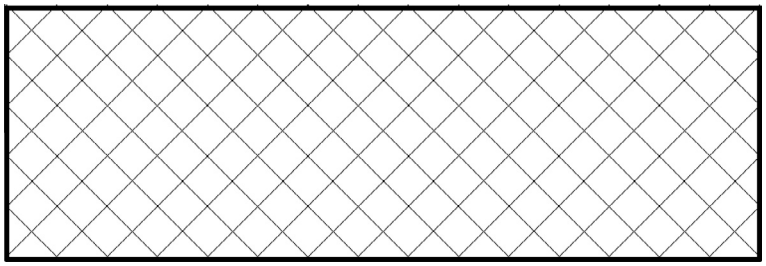

Fig. 2. Reference configuration of a specimen of fibrous composite reinforcement for a bias-extension test.

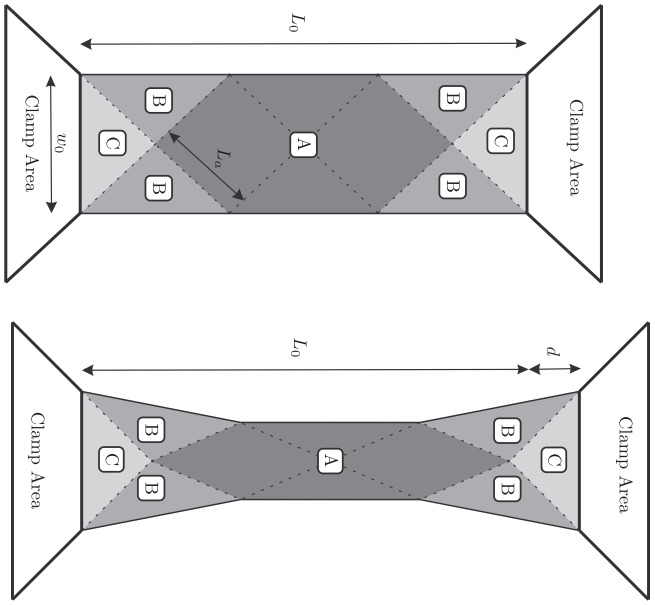

Fig. 3. Simplified description of the deformation pattern in the bias extension test.

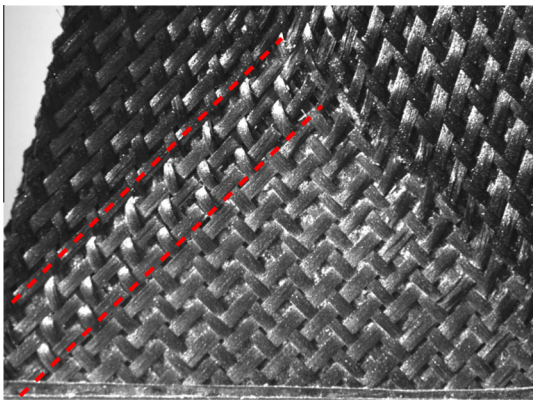

Fig. 4. Shear transition layers in a fibrous composite reinforcement subjected to a bias extension test.

simulations in which this pantographic lattice is used to model a bias extension test and we will discuss the obtained results.

The reason for which the presented discrete lattice cannot be regarded as an always effective model of the fiber reinforcements considered e.g. in Cao et al. (2008) is simple. Indeed, it is true that the fibers which form these fabrics may effectively be individually modeled as beams and that their contact can be in some circumstances be modeled as pivots (see e.g. Wang et al., 1999): however, as they have a section whose diameter can be comparable with the distance between two closest contact zones, the model of Euler beam does not seem always applicable for describing their behavior when they are included in woven fabrics. On the other hand, in the next subsection, we present a structure constituted by elasticae whose section is small when compared to the distance between the closest introduced pivots which are inter-connecting them, so that every fiber can be always effectively modeled as Euler beam.

3.2. Truss Penalty Model

A second way to model networks of almost inextensible yarns is the Truss Penalty Model (TPM). The discretization of the problem is obtained by constraining in a suitable way a standard quadrilateral shell element available in a software like ADINA. In particular, we choose to constrain a quadrilateral shell finite element by means of two rigid bars which are connected to the corners of the element by means of internal pivots (see Fig. 7). The rigid diagonal bars are not connected by an internal hinge at their intersection, as for the pantographic lattices case, but they are free to slide in a relative motion (see Fig. 6). We call the obtained finite element TPM-2. We choose this kind of finite element because it is very robust and accurate. Moreover, this finite element is formulated with a full quadrature scheme (using all Gauss points) so in this way a specific strategy to control the in-plane hour-glass mode is not necessary. It is worth noting that, this kind of finite element is a shell-element, but in this numerical investigation the out-of-plane displacement of the element are forbidden and then the rotational degree of freedom are not activated for the plane geometry and in-plane load condition considered. Summarizing, only the in-plane deformation part is considered and the inextensibility constraint in the fiber direction is accounted for by adding rigid bars as diagonals of the finite element. The introduction of the diagonal truss element constraint penalizes some deformation modes of the finite element: in particular, the global shear deformation mode with respect to the spatial reference frame at the element level.

The admissible deformation modes associated to TPM-2 elements are depicted in Fig. 6: it can be noticed that the presence of the diagonal rigid bars forbids the classical shear modes of the element thus reducing the degrees of freedom from 8 to 6. We can summarize with reference to Fig. 6 by saying that the TPM-2 element only allows the three rigid modes (1,2,3), the extensional deformation mode (4) and the two hour-glass deformation modes (5,6). The introduced penalty method can be interesting for further developments oriented towards the design of specific finite elements. For example, it is possible to conceive a quadrilateral finite element in which the inextensibility constraint along the two diagonals can be implicitly formulated, adopting a reduced integration scheme to overcome the in-plane shear locking and adopting a stabilization strategy for the hour-glass modes analogously to Hamila and Boisse (2013) and Hamila and Boisse (2013), (or introducing in-plane bending stiffness). In the numerical simulations based on the TPM-2 elements which will be presented in the next section,

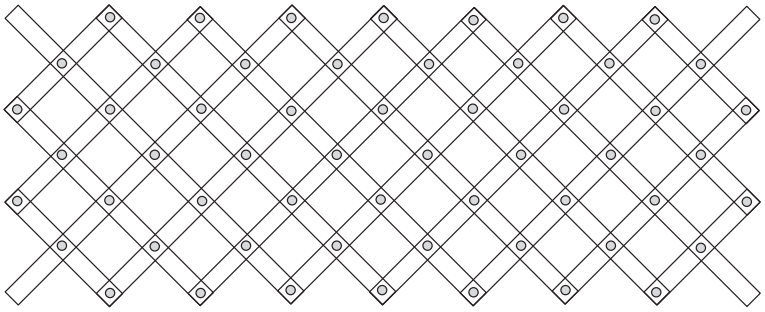

Fig. 5. Module of the pantographic lattice.

Table 1
Properties of the bars constituting the pantographic lattice.

E (Gpa)	ν (–)	D_1 (mm)	D_2 (mm)
6	0.3	1.5	0.6

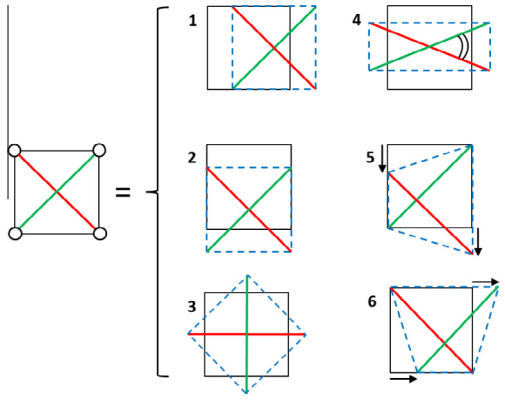

Fig. 6. TPM-2: deformation modes for the base cell obtained by means of the constrained finite element.

the considered constitutive model for the bars is simply linear elastic. Table 2 summarizes the values used for the Young modulus E_m of the membrane, for the Young modulus E_b of the internal bars and for the corresponding Poisson ratios ν_m and ν_b. Moreover, the diameter D of the bars is also given in this table. This linear constitutive assumption will be shown to be sensible for relatively small imposed displacements, but will be seen to be too restrictive to describe the bias extension test for high imposed displacements of the top surface.

The main advantages of this strategy used to account for the inextensibility conditions are: (i) the numerical implementation is very easy to be performed, (ii) the inextensibility condition is not imposed locally at the Gauss points, but a global formulation of the inextensibility conditions is considered for the whole finite element, and (iii) it is possible to obtain a parametric modulation of the stiffness of the constraining bars in order to obtain solutions which are close to the experimental deformed shapes. On the other hand, only linear constitutive equations have been implemented in this model for the sake of simplicity. This fact limits the

Table 2
Elastic properties of the TPM-2 bars.

E_m (MPa)	E_b (GPa)	ν_m (–)	ν_b (–)	D (mm)
0.168	20	0.3	0.3	0.6

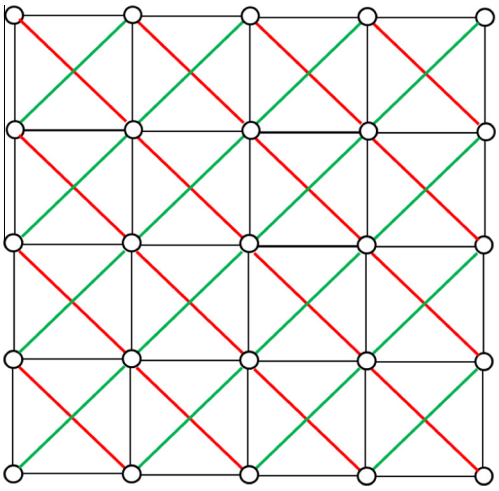

Fig. 7. A periodic modular pattern of TPM-2 discretization (2-family inextensible directions).

applicability of the TPM-2 to the case of imposed displacements of the top surface which only activate geometric non-linearities and not material ones. Indeed, as it will be more deeply discussed, geometrical non-linearities are not sufficient to describe large shear angle variations in the bias test which are associated to high displacements of the top surface. In order to catch such strongly non-linear behavior, material non-linearities have also to be introduced in the constitutive model.

Notwithstanding these limits of the considered TPM-2 finite element for what concerns the highly non-linear regime, we show that it is indeed well adapted to describe the overall behavior of 2D fibrous composites at moderate strains. Of course, a generalization of the considered FE including the possibility of material non-linearities is possible, but is not attempted in the present paper. Such generalization would, in fact, lead to the difficulty of choosing the correct material behavior and, in a second time, induce a long procedure of calibration of the introduced parameters to fit at best the experimental behavior at high strains. The main task of the present paper being that of showing the limits of the considered discrete model with respect to the description of the observed transition layers, we limit ourselves to consider a simplified linear case.

4. Equilibrium shapes of introduced discrete systems

In this section we show the results of the numerical investigations obtained with the different discrete methods presented above. In the next sections, we will instead present two continuum models which will be seen to be better adapted than the discrete ones to the description of the mechanical behavior of 2D fibrous

composites also at high strains. In Fig. 8 we schematically present the three different approaches which we use in this paper to simulate the bias extension test: two particular discrete systems and a continuum approach. The characteristic sizes of the specimen are the same for all numerical simulations treated in this paper:

- basis: 100 mm
- height: 300 mm

In this section we show the strong and weak points of the proposed discrete approaches and we leave to the following sections the treatment of the bias extension test by means of continuum theories.

4.1. Pantographic lattices

Employing the discrete pantographic lattice model introduced in Section 3.1, we compute the equilibrium shape of the specimen subjected to an imposed displacement of the top surface. Fig. 9 displays the current configuration of the testing sample for an imposed displacement of 55 mm: the color distribution indicates, for each yarn, the angle variation field of the yarn itself with respect to its reference configuration. In particular, we can see that the three characteristic regions denoted by A, B and C in Fig. 3 are recovered in the considered discrete numerical simulation. The portion of yarns lying in the triangle C basically stay undeformed and indeed the angle rotation of each fiber with respect to its reference configuration is vanishing as it can be easily deduced from Fig. 9. The two orders of fibers lying in the region A actually rotate of the same amount (almost 20°) with respect to their reference configuration: this is equivalent to say that the total angle variation in the region A is of almost 40°. The situation is slightly different for the portion of yarns lying in the region B. Indeed, it can be recognized that one order of yarns almost remains parallel to the reference configuration (no angle variation). On the other hand, the second order of fibers rotates of almost 20° with respect to the reference configuration: this means that the total angle variation in the region B is of almost 20°. Clearly, it is possible to directly relate the angle variation to the in-plane cross-section rotation of beams due to the fact that the beams are bending in a small transition zone from one triangle at constant shear strain to the adjacent one. Indeed, it is possible to remark that in Fig. 9 the presence of the so called shear transition layer can be detected. The thickness of this transition layer is directly related to the in-plane bending stiffness of fibers. The performed numerical simulations on the pantographic lattice structure allow us to conclude that the presence of the shear transition layer at the macroscopic level is indeed naturally stemming from the particular mesostructure of the considered medium. In particular, we are able to claim that the onset of such transition layers is due to the fact that the shear angle gradually varies from one constant value to another constant value: this variation is made in a thin transition zone in which a rapid gradient of the shear angle variation can be observed. The thickness of such transition layers is clearly related to the in-plane bending stiffness of the fibers. These observations fit with the theoretical results presented in dell'Isola and Steigmann (2014) in which a direct relationship between the in-plane bending strain of fibers and the gradient of shear strain is found. It is hence possible to claim that, in this context, the need of a higher gradient theory is directly stemming from microstructural effects.

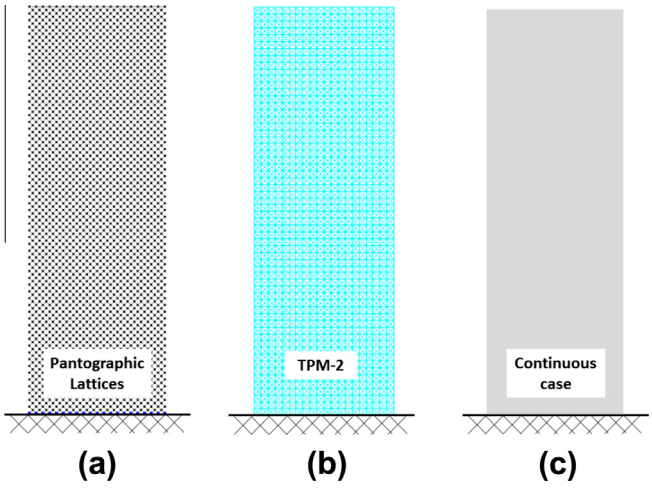

Fig. 8. Schematic representation of the bias extension test simulated with the discrete and continuum models. Basis: 100 mm, height: 300 mm.

Fig. 10 shows the bending energy and the axial energy of the pantographic lattice, respectively. As we could expect, it can be noticed that the bending energy is concentrated in the shear transition layer which determines the transition between two regions at constant shear angle. On the other hand, the axial energy is concentrated on few beams close to the corners of the specimen.

4.2. TPM elements: mesh-dependence of the thickness of the shear transition layer

In Fig. 11, we consider the set up for the problem in study by means of TPM-2 finite elements.

We remark that, in virtue of symmetry, we are able to implement only one fourth of the structure (see Fig. 11). Fig. 12 shows simultaneously the undeformed configuration for the TPM-2 material, the deformed one and a schematic representation of the solution for the bias test in which the three zones at constant shear angle are indicated here as 1, 2 and 3 (see also Fig. 3). Large deformation assumption is accounted for in the numerical simulations only because of geometrical non-linearities. More precisely, the constitutive relations for the single beams are the classical linear-elastic ones (quadratic energy in the deformation measures), but the considered strain measures are nonlinear.

The obtained solution (Fig. 12(b)) reproduces quite precisely the solution for the bias test on a fibrous composite reinforcement, at least for imposed displacements up to 50–55 mm. The obtained solution presents the previously discussed three different zones at constant shear angle: these zones being characterized by a homogeneous deformation process, they show constant strain (or stress) field. It is worth noticing that the representative deformation modes which allow for the transition from one region to the adjacent one are the hour-glass deformation modes 5 and 6 as indicated in Fig. 6. More particularly, these deformation modes are also influenced from the imposed boundary conditions which indeed fix two of the four sides of the TPM-2 elements which remain undeformed. In this context, it is evident how the thickness of the transition layer which is responsible of the transition between two zones at constant shear angle strongly depends on the size of the chosen elements: the transition always occurs on one and only finite element. This fact is underlined in Fig. 13 in which the transition deformation strips are highlighted by means of a different color. This fact must systematically be taken into account when looking for FEM solutions for the bias extension test: a model in which each finite element deforms independently of the deformation of the adjacent ones cannot account for the description of the transition zone in which high gradients of the shear angle variation occur.

The three in-plane Cauchy stress components obtained by means of the TPM-2 model are shown in Fig. 14. In this figure

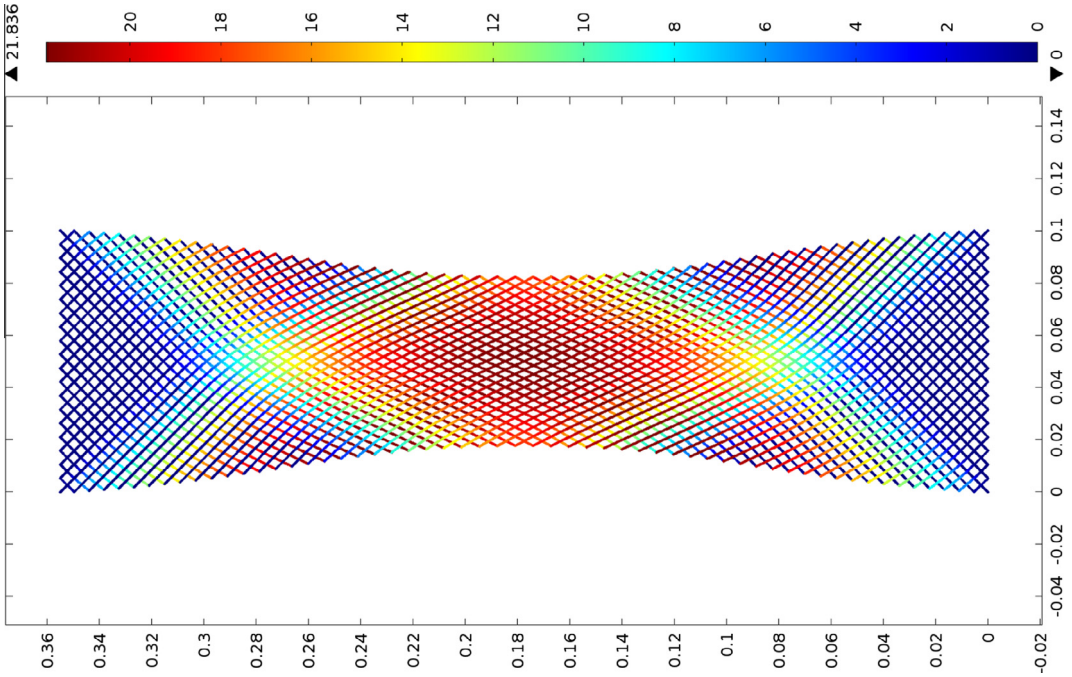

Fig. 9. Fiber angle variation in the pantographic lattice for a displacement of 55 mm.

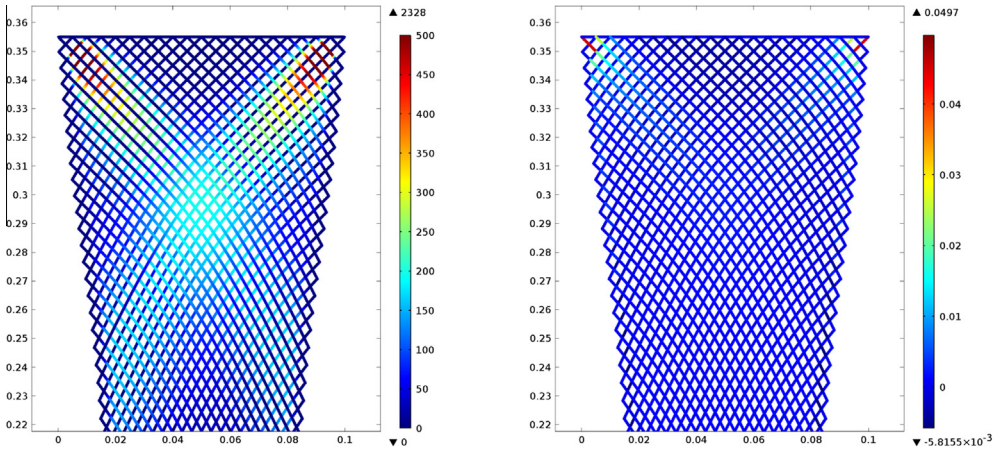

Fig. 10. From left to right: bending energy (J/m) and axial energy (J/m) of the pantographic structure.

one can appreciate the homogeneity of the response and the high strain jumps corresponding to the two transition zones are also evident. Furthermore, we observe that in the limit of very high axial stiffness for the truss there are strong concentrations of the reaction forces in the corners of the specimen, as it is indicated in Fig. 15: all the other reactions are negligible in comparison with respect to those which are highlighted in this picture. This is coherent with the results obtained by means of the panthographic structure model. We explicitly remark that the main features of the obtained response strongly depend on the ratio between the stiffness of the internal diagonal truss and that of the membrane. When decreasing the truss stiffness, all the observed peculiarities of the solution vanish and a standard elastic solution is recovered.

In fact, as it is depicted e.g. in Fig. 16, decreasing the stiffness of the truss of the TPM-2 discretization, the strong gradients disappear compared to the previous high stiffness case. Analogously, the strong concentration at the corners of the reaction field disappears as well. These results allow us to deduce that the typical solution of the bias extension test in which three zones at constant shear angle are present, is indeed deeply related to the strong contrast between the high tensile stiffness of the yarns and the low shear angle variation stiffness. Consequently, this strong contrast of the mechanical properties at the mesoscopic level is also responsible for the onset of shear transition layers between the transition zones: these transition zones cannot be properly taken into account by the considered TPM-2 model. As suggested by the homogenization techniques proposed in Alibert et al. (2003), when considering truss structures with strong contrasts of the mechanical properties, one possible solution to correctly model the structure itself is to consider a second (or higher) gradient continuum model. In the light of these considerations, we are led to the conclusion that one possible strategy for the correct modeling of 2D woven fabrics is indeed that of considering a generalized continuum theory which allows for the description of high strain gradients concentrated in thin transition layers. The development of such continuum theory will be presented in the next section.

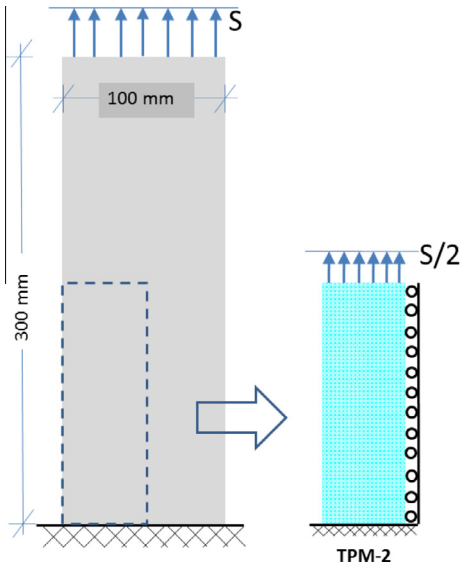

Fig. 11. Set up of the problem and its discretization by TPM-2 mesh.

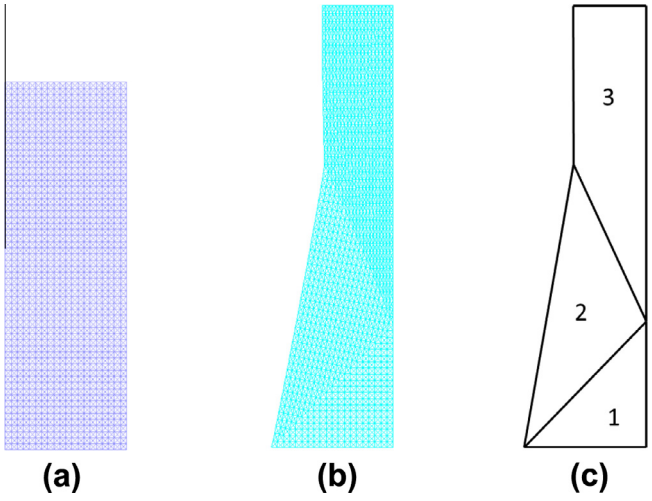

Fig. 12. Initial configuration (a); final configuration (b); homogeneous strain zones (c).

In summary, the TPM-2 model is able to catch the basic features of the bias extension test, but it is not able to correctly describe the thickness of shear transition layers. The geometric non-linearities included in the TPM-2 model allow us to test here the material behavior for imposed displacements up to 55 mm. The solutions obtained by means of the proposed finite elements are reliable and no tension locking problems are encountered.

5. Generalized continuum modeling of fibrous composite reinforcements

In this section we introduce and discuss the interest of using continuum models for the description of the mechanical behavior of fibrous composite reinforcements, also by comparison with the previously discussed discrete numerical simulations. Continuous approaches have been widely used in the last decades to model such class of engineering materials (see e.g. Badel et al., 2009; Boisse et al., 2011; Hamila and Boisse, 2013; Wang et al., 1999; Lomov and Verpoest, 2006; Willems et al., 2008; Yu et al., 2005; Duhovich et al., 2011; Gereke et al., 2013; King et al., 2005). Nevertheless, when modeling with a continuum theory materials which have strong discontinuities of the mechanical properties at the microscopic scale, then a standard Cauchy continuum theory may not be sufficient to fully describe their mechanical behavior at the homogenized scale (see Alibert et al., 2003). This is the case for woven composite reinforcements, at least for certain cases in which particular boundary and/or loading conditions are applied to the considered specimen. Indeed, an orthotropic, first gradient, constitutive law which is able to account for the presence of privileged directions with very high tension stiffness, is not sufficient to catch all the characteristic deformation patterns which woven fabrics may experience. In order to describe the experimentally observed shear strain high gradients related to the bending of fibers at the mesoscopic level, one has to complete the orthotropic continuum model by considering a generalized, second gradient, continuum theory.

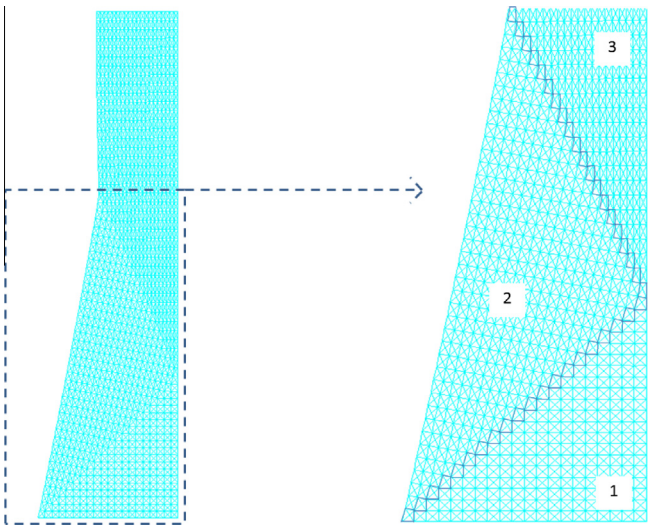

Fig. 13. Transition deformation zones.

The anisotropic behavior of woven composites, due to the presence of very stiff yarns in the warp and weft directions, can be modeled in a continuum framework by means of well established representation theorems (see e.g. Raoult, 2009; Ferretti et al., 2013; Charmetant et al., 2011; Charmetant et al., 2012 and references there cited). These theorems state that orthotropic material behaviors can be described in a continuum framework by choosing constitutive relations which express the strain energy density as function of some invariants of the Cauchy-Green deformation tensor which also take into account the presence of particular orthotropic directions. In particular, for an in-plane 2D problem the quoted orthotropic invariants can be introduced as

$$i_4 = \mathbf{m}_1 \cdot \mathbf{C} \cdot \mathbf{m}_1, \quad i_6 = \mathbf{m}_2 \cdot \mathbf{C} \cdot \mathbf{m}_2, \quad i_8 = \mathbf{m}_1 \cdot \mathbf{C} \cdot \mathbf{m}_2, \tag{1}$$

where $\mathbf{m}_1$ and $\mathbf{m}_2$ are orthonormal vectors in the warp and weft directions, $\mathbf{C} = \mathbf{F}^T \cdot \mathbf{F}$ is the classical Cauchy-Green deformation tensor and $\mathbf{F} = \nabla \boldsymbol{\chi}$ is the gradient of the placement map $\boldsymbol{\chi}$. Clearly, the displacement field can be also introduced as a function of $\boldsymbol{\chi}$ as: $\mathbf{u} = \boldsymbol{\chi} - \mathbf{X}$, where $\mathbf{X}$ is the Lagrangian position of material particles in the reference configuration Ω of the body. It is worth noticing that the first two invariants i_4 and i_6 are related to changes of length in the directions $\mathbf{m}_1$ and $\mathbf{m}_2$ respectively, while the invariant i_8 is a measure of the angle variation between two yarns. Indeed, it can be checked that the total angle variation γ of two superimposed yarns with respect to the reference configuration can be directly related to the introduced invariants by means of the relation

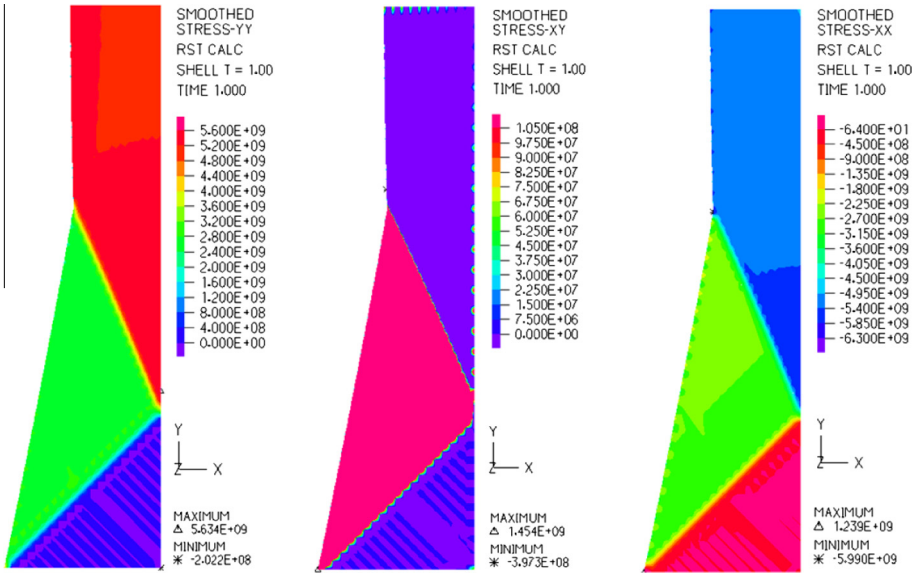

Fig. 14. Stress components of the membrane obtained by means of the TPM-2 discretization approach: σ_{YY} (left), σ_{XY} (center), σ_{XX} (right).

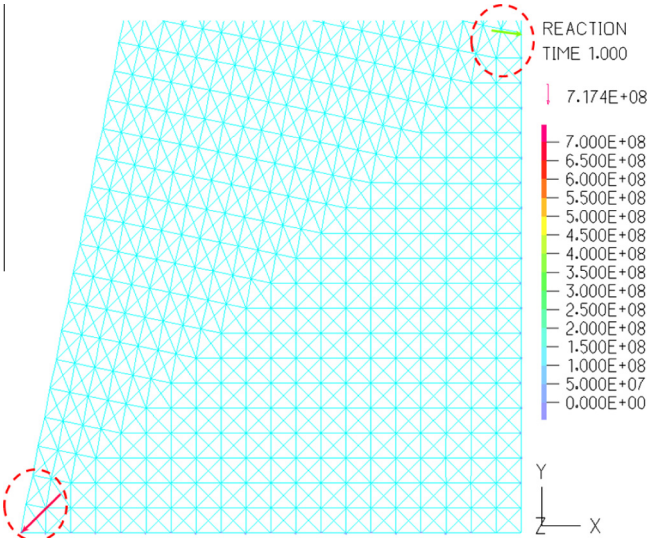

Fig. 15. Reactions force concentration in the TPM-2 model.

$$\gamma = \arcsin\left(\frac{i_8}{\sqrt{i_4 i_6}}\right).$$

It is worth noticing that when one wants to consider orthotropic materials which experience plastic deformations, then an evolution of the considered anisotropy should be taken into account. This would lead to the definition of a more general constitutive framework with respect to the one considered in this paper (see e.g. Cuomo and Fagone, 2009). Different 2D orthotropic materials can be modeled by choosing particular constitutive expressions of the strain energy density in terms of the three introduced invariants. Indeed, orthotropic constitutive relations are able to account for the presence of an orthotropic mesostructure in the considered continua, but they are not able to fully describe the effect of this mesostructure on the macroscopic deformation of the continuum when concentrations of stress and strain occur. For example, it has already been remarked that, when considering the bias extension test, thin transition layers exhibiting concentration of strain appear at the transition between two regions at constant shear

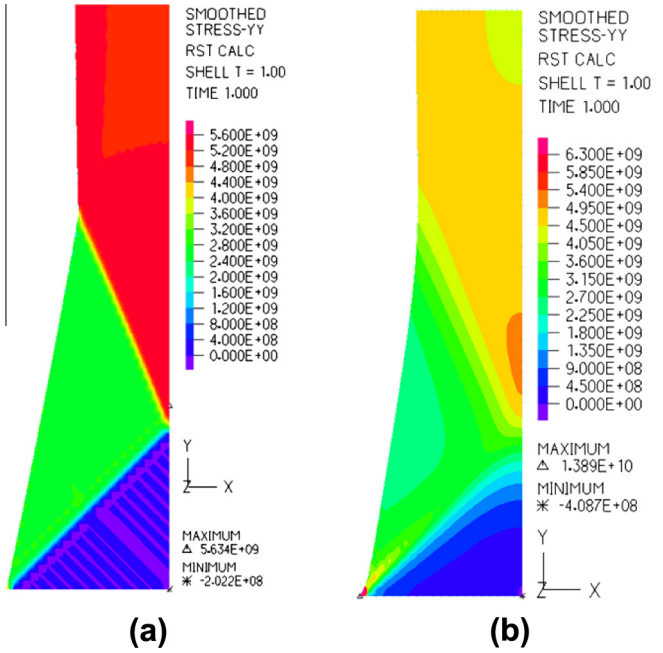

Fig. 16. TPM-2 Model: (a) High diagonal truss stiffness; (b) Low diagonal truss stiffness.

angle. We also remarked, on the basis of the discrete models presented in the present paper, that the thickness of these transition layers is directly related to the bending stiffness of the fibers. Moreover, when considering the TPM-2 element, we highlighted the fact that the size of the shear transition layer is directly related to the size of the considered mesh. On the other hand, when considering the pantographic structure, the size of the transition layer is seen to be well described and to directly depend on the bending stiffness of considered beams. In order to be able to describe the onset of shear transition layers in the framework of a continuum theory, higher gradient theories are known to be needed. On the basis of the quoted remarks and of other phenomenological considerations on the bias test, the constitutive expression of the strain energy density considered in this paper is of the form

$$W = \frac{K_4}{2}(i_4 - 1)^2 + \frac{K_6}{2}(i_6 - 1)^2 + \frac{K_8}{2}(i_8)^2 + \frac{A_8}{2}(i_8)^8 + \frac{\alpha}{2}\nabla i_8 \cdot \nabla i_8. \tag{2}$$

The coefficients K_4 and K_6 represent the tensile rigidity in the $\mathbf{m}_1$ and $\mathbf{m}_2$ directions respectively, K_8 is the shear angle variation stiffness which is valid for small strains (up to an imposed external displacement of 55 mm) and A_8 is instead the shear stiffness for the non-linear regime (external displacements higher than 55 mm). Finally, the coefficient α is the second gradient elastic coefficient which allows to account for high gradients of the shear angle variation and which is capable to describe the onset of shear transition layers.

5.1. Principle of virtual powers and equations in weak form

In this subsection, the least action principle needed to describe the mechanical behavior of fibrous composite reinforcements in the quasi-static regime is set up. In particular, the action functional for our generalized orthotropic continuum can be written as

$$\mathcal{A} = \int_\Omega W(i_4, i_6, i_8, \nabla i_8)\, d\Omega,$$

where Ω is the volume occupied by the fibrous specimen in its reference configuration and the constitutive expression for the strain energy density W is given in Eq. (2). It is worth noticing that considering this expression for the action functional, we are implicitly assuming that all inertial effects can be neglected and that the phenomenon that we are studying can be considered to be quasi-static. As classically done, the power of internal forces of the considered generalized continuum can be written as the first variation of the action functional as: $\mathcal{P}^{int} = \delta\mathcal{A}$. Relying on the principle of virtual powers we can hence write the governing equations for the considered fibrous system in the following weak form

$$\delta\mathcal{A} = \mathcal{P}^{ext}, \tag{3}$$

where $\mathcal{P}^{ext}$ is the power of external forces that, in the framework of the considered second gradient model, we choose to take the particular form

$$\mathcal{P}^{ext} = \int_{\partial\Omega} \left(\mathbf{f}^{ext} \cdot \delta\mathbf{u}\right) + \int_{\partial\Omega} (\tau_4 \cdot \delta i_4 + \tau_6 \cdot \delta i_6 + \tau_8 \cdot \delta i_8),$$

where $\delta\mathbf{u}$ is the virtual displacement field, while δi_4, δi_6 and δi_8 are the virtual variations of the three invariants introduced in Eq. (1). The virtual variations of these invariants can clearly be expressed in terms of the virtual variation of displacement and of its space derivatives by means of the definitions (1). The quantities τ_4, τ_6, and τ_8, represent the external actions expending power on the elongation of the two orders of fibers and on the shear angle variation respectively, while $\mathbf{f}^{ext}$ is the classical surface external force.

5.2. Numerical simulations

The numerical simulations of the continuum model presented in the previous subsection are intended to be directly implemented in the weak form (3) by using the code COMSOL Multiphysics. Indeed, in order to improve the stability of the numerical simulation, the second gradient simulations are implemented via the constrained micromorphic approach presented in Ferretti et al. (2013) to which, to the sake of simplicity, we refer for details on the relation between second gradient and constrained micromorphic theories. Indeed, it is known that second gradient theories can be obtained as suitable limits of micromorphic theories subjected to precise kinematical restrictions (see e.g. Bleustein, 1967; Madeo et al., 2013; Neff et al., 2013a,b).

Table 3
First and second gradient constitutive parameters for the considered orthotropic continuum model.

K_4 (GPa)	K_6 (GPa)	K_8 (MPa)	A_8 (MPa)	α (MPa m^2)
6	6	0.0428	0.18	2×10^{-5}

Table 3 shows the values of the first and second gradient parameters appearing in Eq. (2) which are used in the numerical simulations proposed here. The geometry of the problem in study is of the same type as the one considered in the discrete approaches. More particularly, we consider a rectangular specimen of the same dimensions as the ones considered for the discrete numerical simulations (see Fig. 8). As for the boundary conditions we choose:

- vanishing displacement of the bottom surface ($\delta\mathbf{u} = \{0, 0\}$),
- imposed vertical displacement of the top surface ($\delta\mathbf{u} = \{0, 55\text{ mm}\}$),
- vanishing angle variation at the bottom and top surfaces ($\delta i_8 = 0$),
- vanishing double-tractions at the top and bottom surfaces ($\tau_4 = 0$, $\tau_6 = 0$).

It is worth to discuss with some more details how the aforementioned problem and, in particular, the used boundary conditions have been implemented in the numerical code. The continuum numerical simulations presented in this paper have been performed via the code COMSOL Multiphysics by directly implementing the principle of virtual powers (3). The boundary conditions listed above have been imposed in weak form as well by means of suitable Lagrange multipliers. More precisely, instead of imposing locally that the displacement is vanishing on one side of the specimen, we impose a global integral constraint on the whole line by using a Lagrange multiplier. This approach allows us to directly obtain the value of the resultant reaction force on the basis of the specimen which is indeed directly the value of the introduced Lagrange multiplier. This approach permits to avoid numerical errors in the post-processing phase related to line integrations of the reaction force field on the basis of the specimen.

We start showing the results for the total angle variation obtained via the first and second gradient theory. Indeed, Fig. 17 shows the total angle variation between yarns when imposing a displacement of the top surface of 55 mm. Fig. 18 shows the same quantity obtained by using a second gradient theory. As already proven in Ferretti et al. (2013), it can be seen that when considering the numerical simulation obtained by using a classical first gradient Cauchy theory (see Fig. 17), the solution sensibly deviates from the experimental one, especially for what concerns the description of the shear transition layers. Indeed, as it will be better pointed out in the remainder of this section, the size of the transition layer which is obtained in the framework of a first gradient theory strongly depends on the size of the considered elements. Fig. 18 shows the second gradient solution for the total angle variation: it can be seen that the description of the transition layer is much more accurate and the transition between two zones at constant shear angle actually takes place on smooth transition layers. Moreover, the thickness of the transition layer is seen to be mesh-independent when considering a second gradient theory. Fig. 19 shows in detail how the thickness of the transition layers strongly depend on the size of the considered mesh in the case of the first gradient solution, while Fig. 20 actually shows that this mesh-dependency disappears in the case of second gradient solution when a sufficiently small mesh is considered. It is in fact clear that the characteristic size of the used mesh must be smaller of the thickness of the transition layer in order to obtain the correct solu-

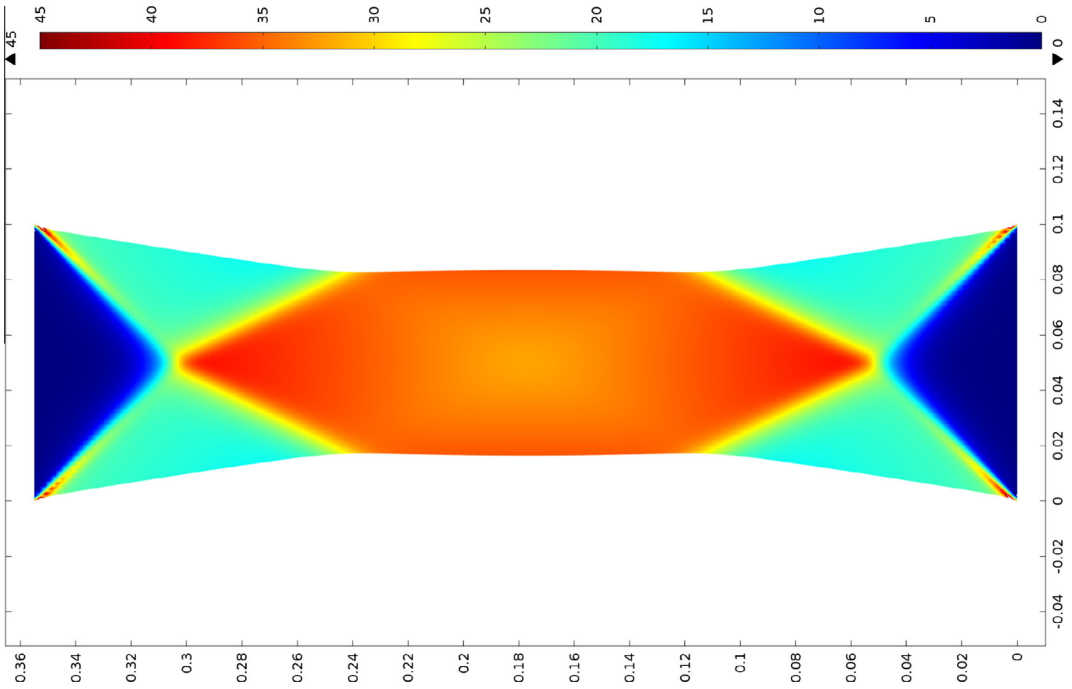

Fig. 17. Total angle variation γ for an imposed displacement of 55 mm: first gradient theory.

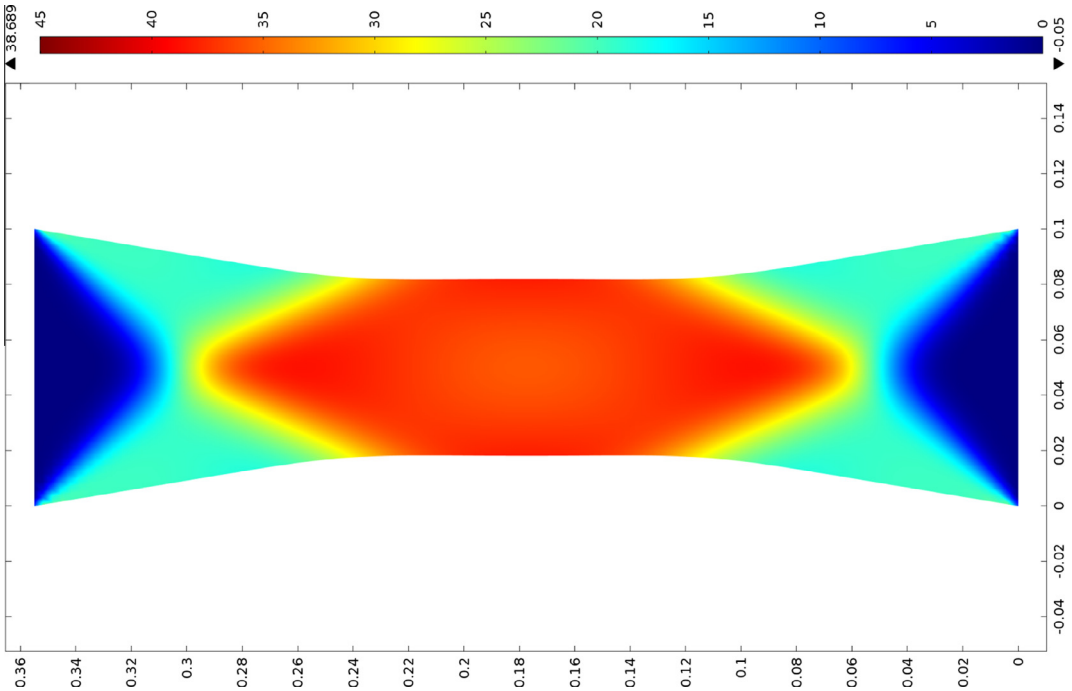

Fig. 18. Total angle variation γ for an imposed displacement of 55 mm: second gradient theory.

tion in the transition layer region. It is for this reason that a sufficiently fine mesh is necessary also in the case of second gradient solution in order to be able to catch the correct solution of the considered problem.

More particularly, it can be remarked that, independently of the size of the considered mesh, in the first gradient solution the thickness of the transition layer is always comparable to the size of one element of the considered mesh (as happened for the TPM-2 solution), while in the second gradient solution, as far as the mesh is small enough to catch the characteristic features of the considered phenomenon, the thickness of the transition layer keeps constant also when considering smaller and smaller meshes. This phenomenon of mesh-dependency is better underlined in Figs. 21 and 22 in which the solution restricted to one section passing across the transition layer is depicted for three different mesh sizes. In these figures the blue line corresponds to the shear angle variation obtained by means of the coarser mesh, while the green and the red line represent the solution corresponding to the medium and the finer mesh respectively. The discussed mesh-independency related to the second gradient solution appears clearly in

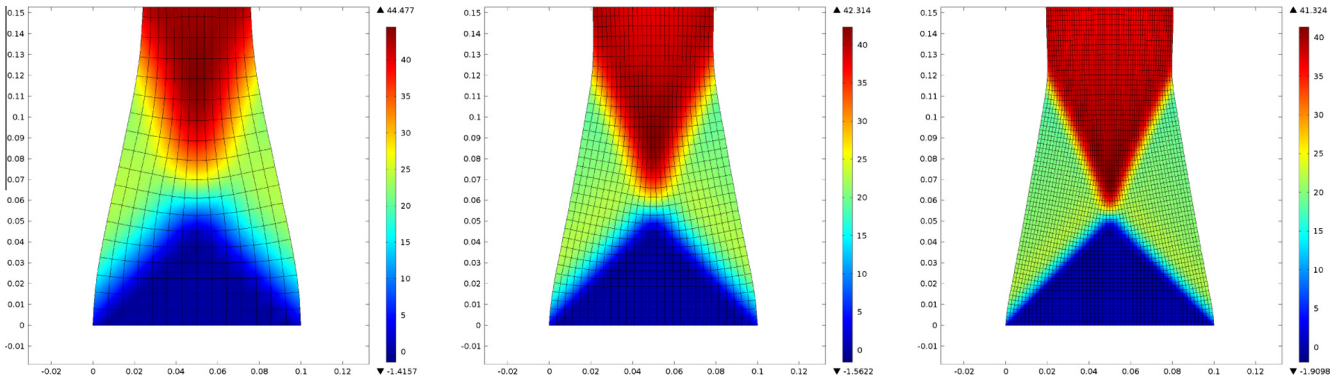

Fig. 19. Dependency of the first gradient solution on the size of the considered mesh.

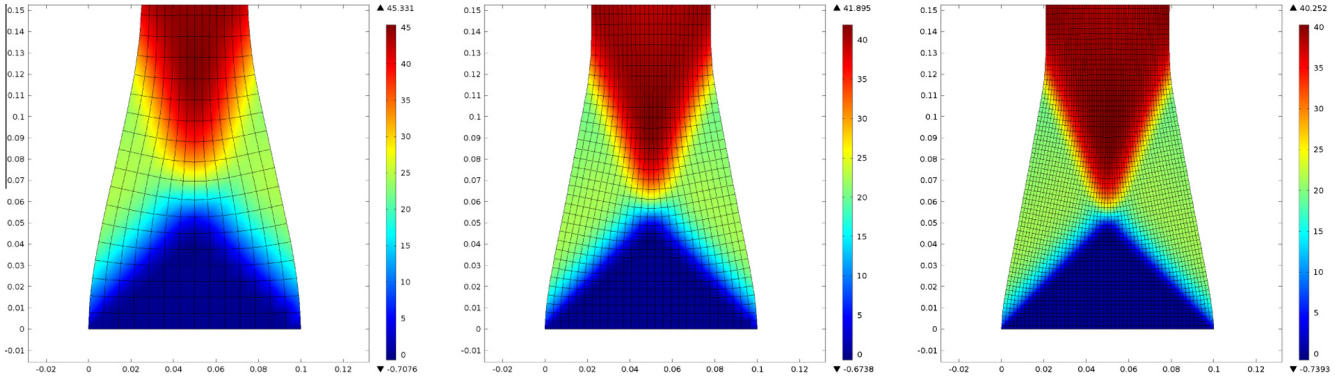

Fig. 20. Independency of the second gradient solution on the size of the considered mesh.

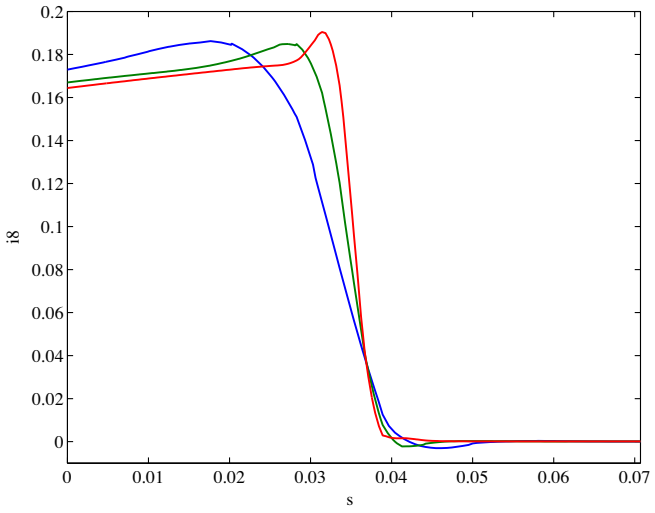

Fig. 21. Dependency of the first gradient solution on the size of the considered mesh.

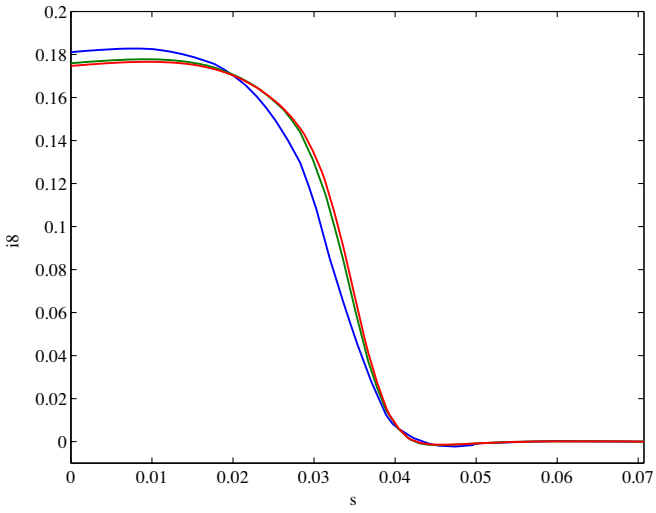

Fig. 22. Independency of the second gradient solution on the size of the considered mesh.

Fig. 22: indeed, the solutions obtained with the medium and finer mesh (green and red lines) are almost perfectly superimposed.

6. Force–displacement curves: discussion about the occurrence of tension locking and comparison of discrete and continuum models

An important physical parameter which directly allows for the comparison of the numerical simulations with the experimental tests is the evolution of the overall force on the bottom surface of the specimen as a function of the displacement imposed at the top surface. Indeed, the force calculated starting from finite element solutions based on continuum models is seen to be often subjected to what is called numerical tension locking (see e.g. Hamila and Boisse, 2013). In particular, the search of a numerical solution for a system which exhibits strong differences between the tension stiffness and the shear angle variation stiffness can lead to numerical errors which give rise to equilibrium configurations in which the fibers appear to be artificially stretched. This implies that the

calculated values of the reaction force on the basis of the specimen appear to be of many orders of magnitude bigger than the expected ones. In Hamila and Boisse (2013) the authors show that the phenomenon of tension locking can be avoided when using bi-linear finite elements, by means of (i) meshes adapted to the directions of the fibers and (ii) stabilization techniques based on reduced integration. Indeed, the phenomenon of tension locking can be also seen to be related to (i) the non-linearity of the considered constitutive behavior and (ii) the type and order of considered finite elements.

Fig. 23 shows that, when considering bi-linear Lagrange square finite elements in the first gradient continuum simulation, the force–displacement curve is over-estimating of three orders of magnitude the expected values of force which is normally included between 0 and 30*N*. When decreasing the mesh size one gets better and better approximation of the calculated force–displacement curve in spite of an increment of calculation time. On the other hand, Fig. 24 shows that when considering quadratic Lagrange elements the convergence to the expected solution is much quicker than in the case of linear elements.

We can summarize by saying that the fact of using continuum theories with constitutive equations of the type (2) in which strong contrasts of the mechanical properties at the mesoscopic level are present, may give rise to numerical errors which are known as tension locking phenomena. This is why the convergence of the calculated solution must always be checked by controlling the corresponding force–displacement curve. The continuum model proposed in the present paper do not show tension locking when considering quadratic elements with a reasonably refined mesh.

Once that the convergence of the continuum solution has been checked, it can be compared with the discrete solutions. Fig. 25 shows the comparison of the force–displacement curve in the linear regime (0–55 mm) as obtained with the pantographic structure, the TPM-2 and the continuum first gradient model respectively. It can be seen that, when considering a range of small imposed displacements ($0 - 55\,mm$), then the discrete models and the first gradient continuum one are all suitable to describe the force–displacement curve for the bias extension test. It is worth to remark that solution obtained with the pantographic lattice slightly overestimates the value of the force and that the force–displacement behavior is perfectly linear. The perfectly linear behavior of the force–displacement curve obtained via the pantographic lattice is related to the fact that the deformation measures

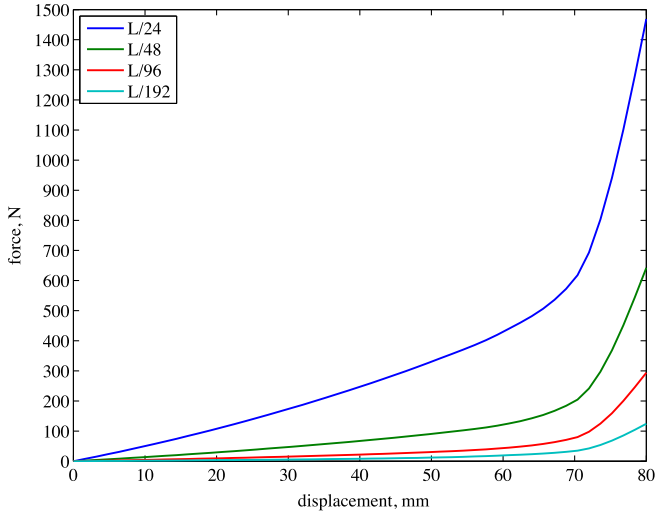

Fig. 23. Comparison of the force–displacement curves for different mesh sizes: the case of bi-linear square finite elements.

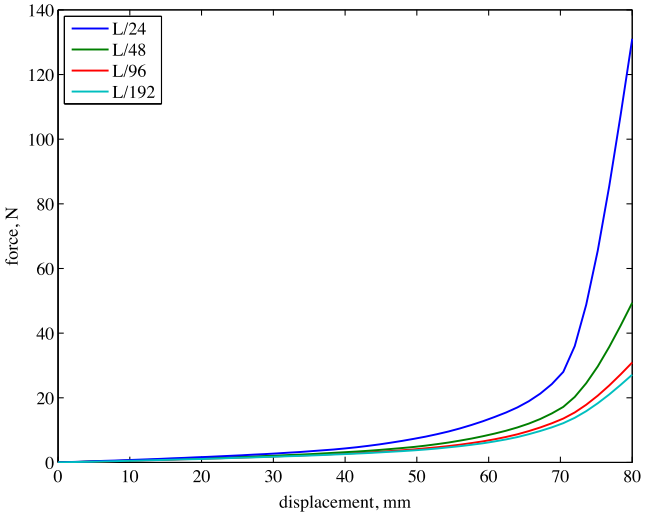

Fig. 24. Comparison of the force–displacement curves for different mesh sizes: the case of bi-quadratic square finite elements.

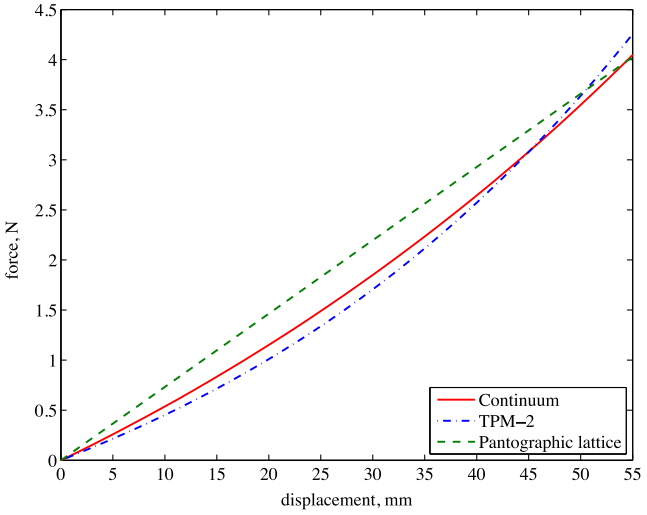

Fig. 25. Comparison of the force–displacement curve obtained via TPM-2 elements and via the continuum first gradient theory: the case of small imposed displacements (up to 55 mm).

of the considered Euler–Bernoulli beams are linearized. On the other hand, the solutions obtained via the TPM-2 and the continuum model show a slightly non-linear behavior which is related to the presence of geometric non-linearities. As already observed, material non-linearities have not been implemented in the pantographic lattice and in the TPM-2 models, while they are taken into account in the continuum model by means of a non-linear constitutive equation for the deformation energy density ($A_8 \neq 0$ in Eq. (2)). Fig. 26 shows the comparison of the first gradient ($\alpha = 0$) continuum solution with linear and non-linear material behavior. The value of the non-linear coefficient A_8 has been calibrated in order to fit at best the experimental force–displacement curve.

Finally, we want to highlight which is the effect of the second gradient constitutive behavior ($\alpha \neq 0$) on the force–displacement curve. To this task, we refer to Fig. 27 in which the first and second gradient solutions are depicted both for the linear and non-linear case. It can be immediately noticed that the global effect of adding a second gradient term in the constitutive equation is that of obtaining a stiffer material, at least for what concerns high imposed displacements. This stiffening effect is much more evident

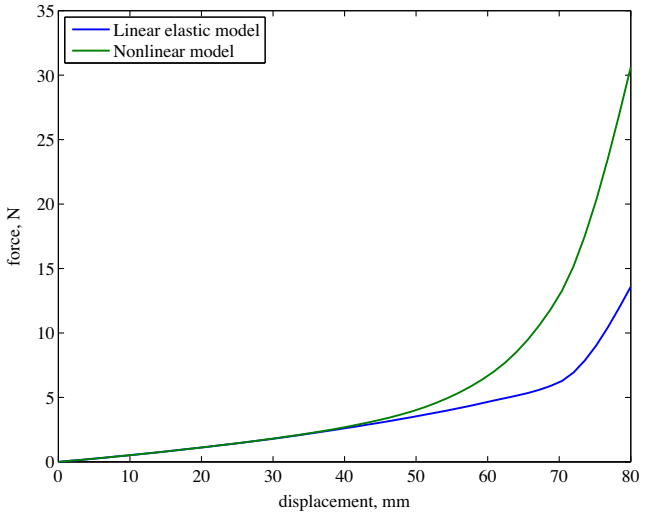

Fig. 26. Force–displacement curves obtained via the continuum first gradient theory: linear and non-linear constitutive assumption.

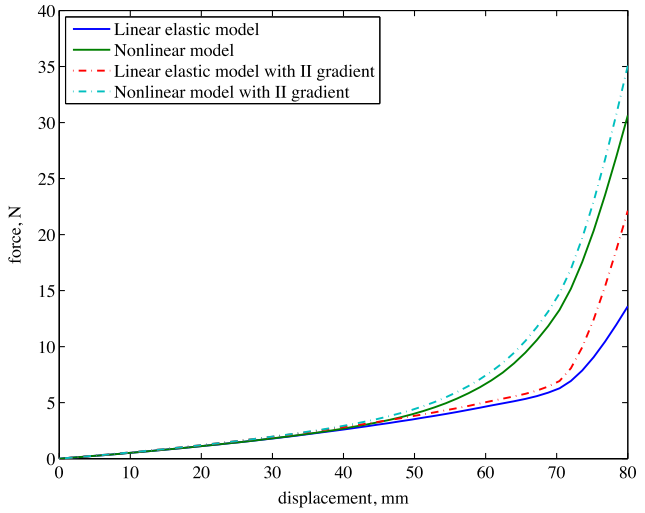

Fig. 27. Force–displacement curves obtained via the continuum first and second gradient theories: linear and non-linear constitutive assumptions.

when considering a linear first gradient model ($A_8 = 0$) than in the non-linear case ($A_8 \neq 0$). The stiffening effect related to second gradient can be associated to the fact that the model accounts for the bending stiffness of the yarns at the mesoscopic level differently to what happens in the first gradient case.

7. Conclusions and perspectives

In this paper it is proven that simple physical mesostructures (which resembles closely some mesostructures used in the technology of fiber reinforced composites) can induce, in the corresponding macroscopic continuum model, a dependence of deformation energy on strain gradient (second gradient theory). The second gradient macroscopic constitutive equation for deformation energy is heuristically determined in terms of the geometry and the mechanical properties of the considered fibrous material. The results obtained in the present paper urge to be rigorously framed in the context of mathematical homogenization techniques of the kind presented in Alibert et al. (2003).

On the basis of the comparison between discrete and continuum models, we conclude that one possible way to correctly describe the behavior of fibrous composite reinforcements is to use a simplified continuum macroscopic description of microscopically complex (i.e. constituted by heterogeneous parts connected following a specific geometric pattern) mechanical systems. One of the main physical feature which leads to conclude that a fibrous composite reinforcement must indeed be modeled as a second gradient continuum is represented by the strong contrast between the very high tensile stiffness of the yarns constituting the lattice and the very low shear angle variation stiffness. Indeed, the yarns of considered woven fabrics can be considered to be almost inextensible, while two superimposed yarns can easily rotate one with respect to the other. In the limit case of inextensibility the introduction of suitable Lagrange multipliers (remarked already by Piola (in preparation)) cannot be avoided. In the present paper we limit ourselves to consider models in which the tensile stiffness of the yarns is much higher than the shear stiffness. The study of the limit case of inextensible networks by the introduction of Lagrange multipliers presents numerous conceptual difficulties which need to be carefully addressed. We henceforth leave the investigation of this delicate case to future work. In this paper, we show how the fact of considering strong contrasts of the mechanical properties at the mesoscopic level actually leads to the conclusion that a second gradient deformation energy must be introduced at the homogenized level. We hence focus on the description of the so-called bias extension test by means of the introduced discrete and continuum models. We find out that:

- The pantographic lattice discrete model is able to account for the description of the basic features of the bias extension test on woven composites, including the description of the onset of shear transition layers. This is possible since each yarn is modeled as a unique Euler–Bernoulli beam with its own bending stiffness: the connection between different beams is realized via perfect internal pivots which do not interrupt the continuity of each yarn. The basic information provided by this discrete model is that if one wants to use a continuum model for the description of the bias extension test, then the possibility of the description of shear transition layers related to the bending stiffness of the yarns at the mesoscopic level must necessarily be taken into account. This result naturally leads to the conclusion that the thickness of the shear transition layers which are observed at the macroscopic scale is indeed directly related to the bending stiffness of the yarns at the mesoscopic scale. This fact must be accounted for when considering a continuum theory for the description of the bias extension test. In particular, following the reasonings presented in dell'Isola and Steigmann (2014), higher gradients of the shear strain must be considered in order to describe the effect of bending stiffness of the yarns on the overall mechanical behavior of the material at the macroscopic level.
- The TPM-2 model is suitable to account for the basic features of the bias extension test, but it shows some limits related to the fact that TPM-2 elements are not actually able to mimic the continuity of yarns. Indeed, the connections between two elements is made by internal pivots, but the bars constituting the rigid truss are not continuous when passing from one element to the adjacent one. This interruption of the continuity of yarns does not create particular problems for the description of the overall behavior of the bias extension test, but it forbids the correct description of the onset of shear transition layers. This limit is related to the fact that no shear angle gradients can be accounted for due to interruption of yarns' continuity. Indeed, we show that the transition from one region at constant shear angle to the adjacent one is made on one single finite

element: non-local bending of fibers is not allowed in the TPM-2 model. This means that the solution is mesh-dependent for what concerns the description of the thickness of the shear transition layers. The main information provided by this discrete model is that when using finite elements, non-local material behaviors must be conceived in order to be able to describe gradual bending of the yarns on more than one element. This information can be added to the preceding ones to conclude that higher order theories are needed for the correct modeling of woven fabrics.

- Continuum models are seen to be suitable to describe in a satisfactory way the basic features of the bias extension test. First gradient models are able to catch most of the features of the considered solution, except for what concerns the correct description of transition layers. Indeed, the thickness of the transition layers predicted by means of the first gradient model strongly depend on the size of the considered mesh (the transition layer is always localized on one element as happened for the TPM-2 model). On the other hand, a second gradient continuum model is able to cure this mesh dependency and the thickness of the shear transition layer remains indeed fixed when decreasing the mesh size. The fact of introducing higher gradients of shear strain in the proposed continuum theory has been seen to be necessary on the basis of precise mesoscopic considerations. In particular the fact of considering such higher gradients of the shear strain allows to account for the bending stiffness of the yarns at the mesoscopic level.

In virtue of the aforementioned remarks, we can conclude that a second gradient continuum model is a possible framework to precisely treat the bias extension test from a theoretical and also from a numerical point of view. Nevertheless, one must be aware of the fact that when looking for finite element solutions of continuum models in which such strong contrasts of the mechanical properties exist, numerical errors related to so-called locking phenomena can be easily introduced (see e.g. Hamila and Boisse, 2013). As a consequence, the numerical integration schemes to be used, in order to apply the formulated model to technologically relevant problems (e.g. bias tests Harrison, 2012; Ten Thije et al., 2007, shear tests Harrison et al., 2008 or (pre) forming of reinforcements Hamila et al., 2009; Badel et al., 2009; Bel et al., 2012; Fetfatsidis et al., 2013; Yu et al., 2005; Duhovich et al., 2011) need to be able to confront the corresponding difficulties. In particular, the convergence of the solution must be carefully checked when considering highly-contrasted media, for example by checking that the obtained solution does not change when refining the mesh of the considered domain.

Further investigations will involve some immediate and interesting developments of presented analysis. These will include the study of:

- pantographic lattices constituted by inextensible fibers by using Lagrange multipliers
- pantographic lattices constituted by different kinds of fibers, having for instance different bending stiffnesses, and showing eventually material gradients of mechanical properties, so that their continuum modeling may require the introduction of inhomogeneous constitutive equations
- more general microstructures with different inextensibility directions in order to more closely aid the design of new meta-materials
- dynamics of pantographic lattices, including eventually phenomena of excitation of internal degrees of freedom (Following the methods used in Boutin et al. (2011) or in Porfiri et al. (2004), Rosi et al. (2010), Porfiri et al. (2005))
- well-posedness properties (e.g. of the kind studied in Jeong and Neff (2010) and Neff (2006)) for the class of nonstandard deformation energies arising in the class of generalized continua we introduced here.

Acknowledgments

This work was partially granted by the Italian Ministry of University and Research (MIUR), under the PRIN 10–11 program, project N. 2010MBJK5B and by INSA-Lyon by means of the BQR project 2013–0054 "Matériaux Méso et Micro-Hétérogènes: Optimisation par Modèles de Second Gradient et Applications en Ingénierie". The authors acknowledge the French MESR for the support to one PhD bourse. We want to finally thank Pierre Seppecher for his invaluable advice, observations, criticism and understanding which were very useful also in this research and to acknowledge fruitful discussions with A. Cazzani, M. Cuomo, V. Eremeyev, S. Federico, A. Grillo, T. Lekszycki, A. Luongo and G. Piccardo on several subjects related to this paper.

References

Alibert, J.-J., Seppecher, P., dell'isola, F., 2003. Truss modular beams with deformation energy depending on higher displacement gradients. Math. Mech. Solids 8 (1), 51–73.

Auffray, N., Bouchet, R., Brechet, Y., 2010. Strain gradient elastic homogenization of bidimensional cellular media. Int. J. Solids Struct. 47 (13), 1698–1710.

Auffray, N., dell'Isola, F., Eremeyev, V., Madeo, A., Rosi, G., in press. Analytical continuum mechanics la Hamilton–Piola: least action principle for second gradient continua and capillary fluids. Math. Mech. Solids. http://dx.doi.org/10.1177/1081286513497616.

Badel, P., Gauthier, S., Vidal-Sallé, E., Boisse, P., 2009. Rate constitutive equations for computational analyses of textile composite reinforcement mechanical behaviour during forming. Compos. Part A: Appl. Sci. Manuf. 40 (8), 997–1007.

Bel, S., Boisse, P., Dumont, F., 2012. Analyses of the deformation mechanisms of non-crimp fabric composite reinforcements during preforming. Appl. Compos. Mater. 19 (3–4), 513–528.

Bleustein, J.L., 1967. A note on the boundary conditions of Toupin's strain gradient-theory. Int. J. Solids Struct. 3, 1053–1057.

Boisse, P., 2012. Composite Fiber Reinforcement Forming. In: Wiley Encyclopedia of Composites, John Wiley and Sons. http://dx.doi.org/10.1002/9781118097298.weoc037.

Boisse, P., Hamila, N., Vidal-Sallé, E., Dumont, F., 2011. Simulation of wrinkling during textile composite reinforcement forming. Influence of tensile, in-plane shear and bending stiffnesses. Compos. Sci. Technol. 71 (5), 683–692.

Bouchet, Auffray N., Brechet, R., 2009. Derivation of anisotropic matrix for bi-dimensional strain-gradient elasticity behaviour. Int. J. Solids Struct. 46 (2), 440–454.

Boutin, C., Hans, S., Chesnais, C., 2011. Generalized beams and continua. Dynamics of reticulated structures. In: Mechanics of Generalized Continua. Springer, New York, pp. 131–141.

Camar-Eddine, M., Seppecher, P., 2002. Closure of the set of diffusion functionals with respect to the mosco-convergence. Math. Models Methods Appl. Sci. 12 (8), 1153–1176.

Camar-Eddine, M., Seppecher, P., 2003. Determination of the closure of the set of elasticity functionals. Arch. Ration. Mech. Anal. 170 (3), 211–245.

Cao, J., Akkerman, R., Boisse, P., Chen, J., Cheng, H.S., De Graaf, E.F., Zhu, B., 2008. Characterization of mechanical behavior of woven fabrics: experimental methods and benchmark results. Compos. Part A: Appl. Sci. Manuf. 39 (6), 1037–1053.

Carcaterra, A., 2002. An entropy formulation for the analysis of energy flow between mechanical resonators. Mech. Syst. Signal Process. 16 (5), 905–920.

Carcaterra, A., Akay, A., 2004. Transient energy exchange between a primary structure and a set of oscillators: return time and apparent damping. J. Acoust. Soc. Am. 115 (2), 683–696.

Cazzani, A., Lovadina, C., 1997. On some mixed finite element methods for plane membrane problems. Comput. Mech. 20 (6), 560–572.

Cazzani, A., Ruge, P., 2012. Numerical aspects of coupling strongly frequency-dependent soil-foundation models with structural finite elements in the time-domain. Soil Dyn. Earthquake Eng. 37, 56–72.

Charmetant, A., Vidal-Sallé, E., Boisse, P., 2011. Hyperelastic modelling for mesoscopic analyses of composite reinforcements. Compos. Sci. Technol. 71, 1623–1631.

Charmetant, A., Orliac, J.G., Vidal-Sallé, E., Boisse, P., 2012. Hyperelastic model for large deformation analyses of 3D interlock composite preforms. Compos. Sci. Technol. 72, 1352–1360.

Ciancio, D., Carol, I., Cuomo, M., 2006. On inter-element forces in the FEM-displacement formulation, and implications for stress recovery. Int. J. Numer. Methods Eng. 66 (3), 502–528.

Contento, A., Luongo, A., 2013. Static and dynamic consistent perturbation analysis for nonlinear inextensible planar frames. Comput. Struct. 123, 79–92.

Contrafatto, L., Cuomo, M., 2005. A globally convergent numerical algorithm for damaging elasto-plasticity based on the Multiplier method. Int. J. Numer. Methods Eng. 63 (8), 1089–1125.

Contro, R., Poggi, C., Cazzani, 1988. A numerical analysis of fire effects on beam structures. Eng. Comput. (Swansea, Wales) 5 (1), 53–58.

Culla, A., Sestieri, A., Carcaterra, A., 2003. Energy flow uncertainties in vibrating systems: definition of a statistical confidence factor. Mech. Syst. Signal Process. 17 (3), 635–663.

Cuomo, M., Contrafatto, L., 2000. Stress rate formulation for elastoplastic models with internal variables based on augmented Lagrangian regularisation. Int. J. Solids Struct. 37 (29), 3935–3964.

Cuomo, M., Fagone, M., 2009. Finite deformation non-isotropic elasto-plasticity with evolving structural tensors. A framework. II Nuovo Cimento C 32 (1), 55–72.

Cuomo, M., Nicolosi, A., 2006. A poroplastic model for hygro-chemo-mechanical damage of concrete. In: Computational Modelling of Concrete Structures – Proceedings of EURO-C 2006, pp. 533–542.

Cuomo, M., Ventura, G., 1998. Complementary energy approach to contact problems based on consistent augmented Lagrangian formulation. Math. Comput. Modell. 28 (4–8), 185–204.

Cuomo, M., Ventura, G., 2002. An explicit formulation of the Green's operator for general one-dimensional structures. Eur. J. Mech. A/Solids 21 (3), 493–512.

Cuomo, M., Contrafatto, L., Greco, L., in press. A variational model based on isogeometric interpolation for the analysis of cracked bodies. Int. J. Eng. Sci.

dell'Isola, F., Steigmann, D., 2014. A two-dimensional gradient elasticity theory for woven fabrics. J. Elast. http://dx.doi.org/10.1007/s10659-014-9478-1.

dell'Isola, F., Rosa, L., Wozniak, L.C., 1997. Dynamics of solids with micro periodic nonconnected fluid inclusions. Arch. Appl. Mech. 67 (4), 215–228.

dell'Isola, F., Rosa, L., Wozniak, L.C., 1998. A micro-structured continuum modelling compacting fluid-saturated grounds: the effects of pore-size scale parameter. Acta Mech. 127 (1–4), 165–182.

dell'Isola, Francesco., Andreaus, Ugo., Placidi, Luca., in press. At the origins and in the vanguard of peri-dynamics, non-local and higher gradient continuum mechanics. An underestimated and still topical contribution of Gabrio Piola. Math. Mech. Solids. Available from: arXiv:1310.5599.

Di Egidio, A., Luongo, A., Paolone, A., 2007. Linear and non-linear interactions between static and dynamic bifurcations of damped planar beams. Int. J. Non-Linear Mech. 42 (1), 88–98.

Duhovich, M., Mitschang, P., Bhattacharayya, D., 2011. Modelling approach for the prediction of stitch influence during woven fabrics draping. Compos. Part A: Appl. Sci. Manuf. 42 (8), 968–978.

Eremeyev, V.A., Pietraszkiewicz, W., 2006. Local symmetry group in the general theory of elastic shells. J. Elast. 85 (2), 125–152.

Eremeyev, V.A., Pietraszkiewicz, W., 2012. Material symmetry group of the non-linear polar-elastic continuum. Int. J. Solids Struct. 49 (14), 1993–2005.

Eringen, A.C., 2001. Microcontinuum Field Theories. Springer-Verlag, New York.

Eringen, A.C., Suhubi, E.S., 1964. Nonlinear theory of simple microelastic solids: I. Int. J. Eng. Sci. 2, 189–203.

Eringen, A.C., Suhubi, E.S., 1964. Nonlinear theory of simple microelastic solids: II. Int. J. Eng. Sci. 2, 389–404.

Federico, S., Gasser, T.C., 2010. Nonlinear elasticity of biological tissues with statistical fibre orientation. J. R. Soc. Interface 7 (47), 955–966.

Federico, S., Grillo, A., 2012. Elasticity and permeability of porous fibre-reinforced materials under large deformations. Mech. Mater. 44, 58–71.

Federico, S., Herzog, W., 2008. Towards an analytical model of soft biological tissues. J. Biomech. 41 (16), 3309–3313. http://dx.doi.org/10.1016/j.jbiomech.2008.05.039.

Federico, S., Grillo, A., Herzog, W., 2004. A transversely isotropic composite with a statistical distribution of spheroidal inclusions: a geometrical approach to overall properties. J. Mech. Phys. Solids 52, 2309–2327.

Ferretti, M., Madeo, A., dell'Isola, F., Boisse, P., 2013. Modeling the onset of shear boundary layers in fibrous composite reinforcements by second-gradient theory. Z. Angew. Math. Phys., 1–26 http://dx.doi.org/10.1007/s00033-013-0347-8.

Fetfatsidis, K.A., Jaures, D., Sherwood, J.A., Chen, J., 2013. Characterization of the tool/fabric and fabric/fabric friction for woven-fabric composites during the thermostamping process. Int. J. Mater. Form. 6 (2), 209–221.

Garusi, E., Tralli, A., Cazzani, A., 2004. An unsymmetric stress formulation for Reissner–Mindlin plates: a simple and locking-free rectangular element. Int. J. Comput. Eng. Sci. 5 (3), 589–618.

Gasser, C., Ogden, R.W., Holzapfel, G.A., 2006. Hyperelastic modelling of arterial layers with distributed collagen fibre orientations. J. R. Soc. Interface 3, 15–35.

Gereke, T., Dbrich, O., Hbner, M., Cherif, C., 2013. Experimental and computational composite textile reinforcements forming: a review. Compos. Part A: Appl. Sci. Manuf. 46 (1), 1–10.

Germain, P., 1973a. The method of virtual power in continuum mechanics. Part 2: microstructure. SIAM J. Appl. Math. 25, 556–575.

Germain, P., 1973b. La mthode des puissances virtuelles en mcanique des milieux continus. Premire partie. Thorie du second gradient. J. Mec. 12, 235–274.

Greco, L., Cuomo, M., 2013. B-spline interpolation of Kirchhoff–Love space rods. Comput. Methods Appl. Mech. Eng. 256 (1), 251–269.

Greco, L., Cuomo, M., 2014. An implicit G^1 multi patch B-spline interpolation for Kirchhoff–Love space rods. Comput. Methods Appl. Mech. Eng. 269 (1), 173–197.

Green, A.E., Rivlin, R.S., 1964a. Multipolar continuum mechanics. Arch. Ration. Mech. Anal. 17 (2), 113–114.

Green, A.E., Rivlin, R.S., 1964b. Simple force and stress multipoles. Arch. Ration. Mech. Anal. 16, 325–353.

Green, A.E., Rivlin, R.S., 1964c. On Cauchy's equations of motion. Z. Angew. Math. Phys. (ZAMP) 15, 290–292.

Green, A.E., Rivlin, R.S., 1965. Multipolar continuum mechanics: functional theory I. Proc. R. Soc. London Ser. A: Math. Phys. Eng. Sci. 284, 303–324.

Hamila, Nahine, Boisse, Philippe, 2013. Tension locking in finite-element analyses of textile composite reinforcement deformation. C.R. Mec. 341 (6), 508–519.

Hamila, N., Boisse, P., 2013. Locking in simulation of composite reinforcement deformations. Analysis and treatment. Compos. Part A 53, 109–117.

Hamila, N., Boisse, P., Sabourin, F., Brunet, M., 2009. A semi-discrete shell finite element for textile composite reinforcement forming simulation. Int. J. Numer. Methods Eng. 79 (12), 1443–1466.

Harrison, P., 2012. Normalisation of biaxial bias extension test results considering shear tension coupling. Compos. Part A: Appl. Sci. Manuf. 43 (9), 1546–1554.

Harrison, P., Wiggers, J., Long, A.C., 2008. Normalization of shear test data for rate-independent compressible fabrics. J. Compos. Mater. 42 (22), 2315–2344.

Holzapfel, G.A., Gasser, T.C., Ogden, R.W., 2000. A new constitutive framework for arterial wall mechanics and a comparative study of material models. J. Elast. 61, 1–48.

Indelicato, Giuliana., 2008. Mechanical models for 2D fiber networks and textiles. Diss. Thse de doctorat LEMTA, Torino, Universit degli studi di Torino, Institut National Polytechnique de Lorraine.

Jeong, J., Neff, P., 2010. Existence, uniqueness and stability in linear Cosserat elasticity for weakest curvature conditions. Math. Mech. Solids 15 (1), 78–95.

King, M.J., Jearanaisilawong, P., Socrate, S., 2005. A continuum constitutive model for the mechanical behavior of woven fabrics. Int. J. Solids Struct. 42, 3867–3896.

Ko, I.M., Carcaterra, A., Xu, Z., Akay, A., 2005. Energy sinks: vibration absorption by an optimal set of undamped oscillators. J. Acoust. Soc. Am. 118 (5), 3031–3042.

Koiter, W.T., 1964. Couple-stresses in the theory of elasticity. Proc. K. Ned. Akad. Wet. B67, 17–44.

Kuznetsov, E.N., 1991. Underconstrained Structural Systems. Springer, Berlin.

Lanir, Y., 1983. Constitutive equations for fibrous connective tissues. J. Biomech. 16, 1–12.

Lomov, S.V., Verpoest, I., 2006. Model of shear of woven fabric and parametric description of shear resistance of glass woven reinforcements. Compos. Sci. Technol. 66, 919–933.

Luongo, A., 1991. On the amplitude modulation and localization phenomena in interactive buckling problems. Int. J. Solids Struct. 27 (15), 1943–1954.

Luongo, Angelo., 1995. Transfer matrix-perturbation approach to the buckling analysis of nonlinear periodic structures. Proc. Eng. Mech. 1, 505–508.

Luongo, A., 2001. Mode localization in dynamics and buckling of linear imperfect continuous structures. Nonlinear Dyn. 25 (1–3), 133–156.

Luongo, A., Pignataro, M., 1988. Multiple interaction and localization phenomena in the postbuckling of compressed thin-walled members. AIAA J. 26 (11), 1395–1402.

Luongo, A., Rega, G., Vestroni, F., 1986. On nonlinear dynamics of planar shear indeformable beams. J. Appl. Mech. Trans. ASME 53 (3), 619–624.

Madeo, A., Neff, P., Ghiba, I.D., Placidi, L., Rosi, G., 2013. Wave propagation in relaxed micromorphic continua: modeling metamaterials with frequency band-gaps. Contin. Mech. Thermodyn. http://dx.doi.org/10.1007/s00161-013-0329-2.

Merodio, J.R., Ogden, W., 2005. Mechanical response of fiber-reinforced incompressible non-linearly elastic solids. Int. J. Non-Linear Mech. 40, 213–227.

Mindlin, R.D., 1964. Micro-structure in linear elasticity. Arch. Ration. Mech. Anal. 16, 51–78.

Mindlin, R.D., 1965. Second gradient of strain and surface tension in linear elasticity. Int. J. Solids Struct. 1, 417–438.

Mindlin, R.D., Eshel, N.N., 1968. On first strain-gradient theories in linear elasticity. Int. J. Solids Struct. 4, 109–124.

Mindlin, R.D., Tiersten, H.F., 1962. Effects of couple-stresses in linear elasticity. Arch. Ration. Mech. Anal. 11, 415–448.

Neff, P., 2006. Existence of minimizers for a finite-strain micromorphic elastic solid. R. Soc. Edinburgh – Proc. A 136 (5), 997–1012.

Neff, P., Forest, S., 2007. A geometrically exact micromorphic model for elastic metallic foams accounting for affine microstructure. Modelling, existence of minimizers, identification of moduli and computational results. J. Elasticity 87 (2–3), 239–276.

Neff, P., Ghiba, I.D., Madeo, A., Placidi, L., Rosi, G., 2013a. A unifying perspective: the relaxed linear micromorphic continuum. Contin. Mech. Thermodyn. http://dx.doi.org/10.1007/s00161-013-0322-9.

Neff, P., Ghiba, I.D., Madeo, A., Placidi, L., Rosi, G., 2013b. A unifying perspective: the relaxed linear micromorphic continuum. Contin. Mech. Thermodyn., 1–43 http://dx.doi.org/10.1007/s00161-013-0322-9.

Oliveto, G., Cuomo, M., 1988. Incremental analysis of plane frames with geometric and material nonlinearities. Eng. Struct. 10 (1), 2–12.

Pideri, C., Seppecher, P., 1997. A second gradient material resulting from the homogenization of an heterogeneous linear elastic medium. Contin. Mech. Thermodyn. 9 (5), 241–257.

Pignataro, M., Luongo, A., 1994. Interactive buckling of an elastically restrained truss structure. Thin-Walled Struct. 19 (2–4), 197–210.

Piola, G., in preparation. Memoria intorno alle equazioni fondamentali del movimento di corpi qualsivogliono considerati secondo la naturale loro forma e costituzione, Modena, Tipi del R.D. Camera, 1846 translated by F.dell'Isola, U. Andreaus, L. Placidi. In: Andreaus, dell'Isola, F., Esposito, R., Forest, S., Maier, G., Perego, U. (eds.), The Complete Works of Gabrio Piola, vol. IU. Springer Verlag (see also <www.fdellisola.it>).

Pipkin, A.C., 1980. Some developments in the theory of inextensible networks. Q. Appl. Math. 38, 343.

Pipkin, A.C., 1981. Plane traction problems for inextensible networks. Q.J. Mech. Appl. Math. 34, 415.

Pipkin, A.C., 1984. Equilibrium of Tchebychev nets. Arch. Ration. Mech. Anal. 85, 81.

Porfiri, M., dell'Isola, F., Frattale Mascioli, F.M., 2004. Circuit analog of a beam and its application to multimodal vibration damping, using piezoelectric transducers. Int. J. Circ. Theor. App. 32 (4), 167–198.

Porfiri, M., dell'Isola, F., Santini, E., 2005. Modeling and design of passive electric networks interconnecting piezoelectric transducers for distributed vibration control, Int. J. Appl. Electrom. 21 (2), 69–87.

Qiu, G.Y., Pence, T.J., 1997. Remarks on the behavior of simple directionally reinforced incompressible nonlinearly elastic solids. J. Elast. 49, 1–30.

Raoult, A., 2009. Symmetry groups in nonlinear elasticity: an exercise in vintage mathematics. Commun. Pure Appl. Anal. 8 (1), 435–456.

Reccia, E., Cazzani, A., Cecchi, A., 2012. FEM-DEM modeling for out-of-plane loaded masonry panels: a limit analysis approach. Open Civil Eng. J. 6 (1), 231–238.

Rosi, G., Pouget, J., dell'Isola, F., 2010. Control of sound radiation and transmission by a piezoelectric plate with an optimized resistive electrode, Eur. J. Mech. A-Solid. 29 (5), 859–870.

Russo, L., 2004. The Forgotten Revolution How Science Was Born in 300 BC and Why It Had to Be Reborn. Springer, Berlin.

Seppecher, P., Alibert, J., dell'Isola, F., 2011. Linear elastic trusses leading to continua with exotic mechanical interactions. J. Phys.: Conf. Ser., 319

Spencer, A.J.M., 1972. Deformations of Fibre-reinforced Materials. Oxford University Press, London.

Spencer, A.J.M., Soldatos, K.P., 2007. Finite deformations of fibre-reinforced elastic solids with fibre bending stiffness. Int. J. Non-Linear Mech. 42, 355–368.

Steigmann, D.J., Pipkin, A.C., 1991. Equilibrium of elastic nets. Philos. Trans. R. Soc. London A335, 419–454.

Svendsen, B., Neff, P., Menzel, A., 2009. On constitutive and configurational aspects of models for gradient continua with microstructure. Z. Angew. Math. Mech. 89 (8), 687–697.

Ten Thije, R.H.W., Akkerman, R., Huetink, J., 2007. Large deformation simulation of anisotropic material using an updated Lagrangian finite element method. Comput. Methods Appl. Mech. Eng. 196 (33), 3141–3150.

Tomic, A., Grillo, A., Federico, S., 2014. Poroelastic materials reinforced by statistically oriented fibres – numerical implementation and application to articular cartilage. IMA J. Appl. Math. 79 (5), 1027–1059.

Toupin, R.A., 1962. Elastic Materials with couple-stresses. Arch. Ration. Mech. Anal. 11, 385–414.

Toupin, R.A., 1964. Theories of elasticity with couple stress. Arch. Ration. Mech. Anal. 17, 85–112.

Wang, J., Paton, R., Page, J.R., 1999. The draping of woven fabric preforms and prepregs for production of polymer composite components. Compos. Part A: Appl. Sci. Manuf. 30 (6), 757–765.

Willems, A., Lomov, S.V., Verpoest, I., Vandepitte, D., 2008. Optical strain fields in shear and tensile testing of textile reinforcements. Compos. Sci. Technol. 68, 807–819.

Yu, W.R., Harrison, P., Long, A., 2005. Finite element forming for non-crimp fabrics using a non-orthogonal constitutive equation. Compos. Part A 36, 1079–1093.